Title
Potential benefits and optimization of cool-coated office buildings: A case study in Chongqing, China

Authors
Zhuang, Chaoqun
Gao, Yafeng
Zhao, Yingru
et al.

Publication Date
2021-07-01

DOI
10.1016/j.energy.2021.120373

Peer reviewed

Potential benefits and optimization of cool-coated office buildings: A case study in Chongqing, China

Chaoqun Zhuang[a,b], Yafeng Gao[a], Yingru Zhao[c], Ronnen Levinson[d], Per Heiselberg[e], Zhiqiang Wang[a], Rui Guo[a,e*]

[a] *Joint International Research Laboratory of Green Building and Built Environment, Ministry of Education, Chongqing University, Chongqing, China*

[b] *Department of Building Services Engineering, The Hong Kong Polytechnic University, Kowloon, Hong Kong, China*

[c] *College of Energy, Xiamen University, Xiamen, China*

[d] *Heat Island Group, Lawrence Berkeley National Laboratory, Berkeley, California, USA*

[e] *Department of the Built Environment, Aalborg University, Thomas Manns Vej 23, Aalborg 9220, Denmark*

**Corresponding author email address: rgu@build.aau.dk*

Abstract

Increasing envelope facet albedos considerably reduces solar heat gain, thus yielding building cooling energy savings. Few studies have explored the potential benefits of utilizing cool coatings on building envelopes ("cool-coated buildings") based on life-cycle cost analysis. A holistic approach integrating the field testing, building energy simulation, and a 20-year life-cycle-based optimization was developed to explore cool-coated building performance and the maximum net savings of optimal building envelope retrofit and design. Experimental results showed that applying cool coatings to a west wall of an office building in Chongqing, China reduced its exterior surface temperature by up to 9.3 °C in summer. Simulation results showed that in Chongqing, making the roof and walls cool could reduce annual HVAC electricity use by up to 11.9% in old buildings (with poorly insulated envelopes) and up to 5.9% in new buildings. Retrofitting old buildings with a cool roof provided the net savings per modified area with present values up to 42.8 CNY/m^2; retrofitting a new building with a cool roof or cool walls was not cost-effective. Optimizing both envelope insulation and envelope albedo can achieve 5.6 times the net savings of optimizing the insulation only, and 1.6 times that of optimizing albedo only.

Keywords:

Cool roof; Cool wall; Life-cycle cost analysis; Optimization; Design; Retrofit

Nomenclature

English symbols

A_i	Area of envelope surface *i* (m^2)
A_m	Total envelope surface area modified (m^2)
$\Delta C_{x,z}$	Cost difference for research case *x* in year *z* (CNY)
e_c	Annual whole-building HVAC electricity savings (kWh)
e_z	Average compounded annual electricity price escalation rate factor in year *z*
E	Annual whole-building HVAC electricity use (kWh)
g	Reduction of annual conduction heat gain intensity (kWh/m^2)
j	Annual electricity savings intensity (kWh/m^2)
N	Number of years in the life cycle
N_p	Number of data points at interval *p*
r_i	Measured data points for model instance *i*
$\Delta S_{x,z}$	Savings for research case *x* in year *z* (CNY)
T	Number of peak-demand hours in a year
w	Annual-average HVAC peak-power demand reduction intensity (kW/m^2)
Y	Net savings (CNY)

Greek

η	Electricity transmission efficiency
ρ_i	Albedo of envelope facet *i*

Abbreviations

AC	Air conditioner or air conditioning
BEPS	Building energy performance simulation
CHG	Conduction heat gain
COP	Coefficient of performance
CO_2	Carbon dioxide
CSV	Comma-separated value
CV(RMSE)	Coefficient of variation of root mean square error
EPS	Expanded polystyrene
GA	Genetic algorithm
HVAC	Heating, ventilation, and air conditioning
IDF	Input data file
LCCA	Life-cycle cost analysis
LST	Local standard time

MAE	Mean absolute error
MBE	Mean bias error
NO_x	Nitrogen oxides
SO_2	Sulfur dioxide
SRHG	Solar radiation heat gain
TMY	Typical meteorological year

1 Introduction

1.1 Background

Improvement of building energy efficiency is one of the key issues to achieve energy conservation and environmental sustainability, as buildings contribute over 40% of primary energy consumption and one-third of global CO_2 emissions worldwide [1]. One of the effective ways to improve the building performance is to select cool surfaces with high albedo (ability to reflect sunlight, spectrum 0.3 – 2.5 μm; also known as solar reflectance) and high thermal emittance (ability to radiate heat, spectrum 4 – 80 μm) [2]. Utilizing cool coatings helps save energy [3] and reduce power-plant emissions of CO_2, SO_2, and NO_x in conditioned buildings [4] and improve thermal comfort in non-conditioned buildings [5] in hot weather, while it may also increase heating demand or result in thermal discomfort in cold weather [6].

Many studies have simulated or measured the direct cooling benefits when applying cool coatings on roofs (cool roofs). Xu et al. [7] measured annual cooling energy savings from roof-whitening of previously black roofs ranging from 14 – 26% in the Metropolitan Hyderabad region (India). Haberl and Cho [8] reported 2 – 44% cooling energy savings and 3 – 35% peak cooling power reduction due to the applications of cool roofs in U.S. residential and commercial buildings. Synnefa et al. [9] estimated that cool roofs reduced discomfort hours by 9 – 100% and the indoor temperature up to 1.2 – 3.3 ºC in non-air-conditioned residential buildings in various climatic conditions. However, when applying cool roofs, the winter penalties are also significant, especially in cold regions where the heating demand is predominant. For instance, Costanzo et al. [10] concluded that an increase in the heating primary energy use might exceed the cooling energy savings when applying a cool roof (albedo 0.85) to an office building in Milan, northern Italy. In another study [11], the application of cool roofs (albedo 0.89) yielded an increase of 43% heating energy in Crete, Greece.

Some researchers also investigated the effects of applying cool coatings on walls (or cool walls). Although exterior walls receive less solar irradiation annually, they typically offer comparable energy savings for three main reasons: (1) Walls have only about half as much insulation as roofs [12]. (2) Wall area is much larger than roof area in most buildings [13]. (3) Cool roofs only affect the thermal performance of rooms on the top floor, while cool walls affect the entire building. Shen et al. [14] measured the impacts of reflective coatings on walls in different orientations in Shanghai. They found that increasing wall albedo to 0.61 from 0.32 resulted in an average reduction of 6 °C of exterior surface temperature on the west wall in summer, and a reduction of 8.3 °C on the south wall in winter. Guo et al. [15] pointed out that in the city of Hangzhou, China, the air-conditioning electricity savings from adopting cool walls on four sides were about 5.8 kWh/(m^2·month), and the maximum exterior wall surface temperature reduction was about 8 – 10 °C. Rosado and Levinson [12] performed over 100,000 whole-building energy simulations to study cool-wall and cool-roof effects in isolated buildings, spanning different building categories, building vintages, and climate zones. They found that cool wall energy savings often equaled or exceeded those from cool roofs because building codes typically prescribe much less wall insulation than roof insulation.

The above studies focus on the energy effectiveness of cool roofs or walls only, while their cost-effectiveness is also an important issue to be addressed. A 20-year life-cycle cost analysis (LCCA) conducted by Saafi and Daouas [16] found that in Tunisia, restored cool roofs (albedo 0.71) achieved a net savings (i.e., deducting the discounted value of the expected costs of an investment from the discounted value of the expected returns) up to USD 15/m^2 with a discounted payback period of 3.4 years, when taking a gray roof (albedo 0.2) as the reference case. Sproul et al. [17] determined that an aged white roof (albedo 0.55) provides a 50-year net savings of USD 25/m^2 compared with black roofs in the US. Shi et al. [18] estimated that installing a cool roof (albedo 0.60) over an existing gray roof (albedo 0.20) yielded 40-year net savings of 5.7 – 35.1 CNY/m^2 (or 0.8 – 5.0 USD/m^2) in warm winter zones in China.

Other studies have explored the effects of roof thermal resistance and roof albedo on building HVAC energy cost. Arumugam et al. [19] found that in India, for a roof with an albedo of 0.6, the optimized roof thermal resistance value is 0.49 m^2·K/W in hot and dry and composite climates, 0.31 m^2·K/W in warm and humid and temperate climates, and 1.02 m^2·K/W for cold climates. Piselli et al. [20] demonstrated high roof albedo (0.80) and no or low insulation yield the minimum HVAC energy consumption in almost all climate conditions worldwide (Sydney, Mexico City, Rome, San Francisco, Rio de Janeiro, and Thessaloniki), except for extremely hot or cold climate zones (Abu Dhabi, New Delhi, Paris, Beijing, Moscow, and Tampere).

One challenge encountered in the applications of cool coatings is that the soiling and weathering contribute to surface albedo losses, which may severely undermine the effectiveness of cool surfaces from a life-cycle perspective. In fact, due to the dust, ultraviolet radiation, microbial growth, rain, wind and biomass accumulation, the albedo of cool surfaces could considerably reduce over time, thus affecting the cooling benefits of cool surfaces. According to Bretz and Akbari [21], most of the decrease in the albedo of cool surfaces occurs in the first year and then the albedo tends to be stabilized. The losses of performance can amount to 20 – 30% of the initial albedo [22]. Several technologies are currently available to prevent or reduce albedo losses due to material aging. For instance, through periodic power washing with water or detergents, the albedo loss could be regained up to 70 – 100% [23]. While the effects of either cool roofs or cool walls on the building energy or economic performance are well investigated in previous studies, the energy- and cost-effectiveness of cool-coated buildings (i.e., combining cool walls and roofs) from a perspective of the life cycle remain a challenge to be addressed.

Over the past decades, building construction in China's urban areas has surged, increasing building stock floor area to 47.3 billion m^2 and 12.8 billion m^2 for residential and public buildings, respectively, by 2018 [24]. China currently accounts for around one-third of global growth in energy used for space cooling with an extraordinary average annual growth rate of 13% [25]. This situation presents many opportunities to specify and apply cool coating products to building envelope under energy-saving policies. In China, the first energy efficiency code for public buildings was developed in 1993 [26]. Since then, new codes have been released periodically, often raising insulation requirements. The newest GB 50189-2015 *Design standard for energy efficiency of public buildings of China* [27] prescribed insulation requirements for exterior walls and roofs more stringent than in previous standards (e.g., GB 50189-93 [26] and 50189-2005 [28]). Public buildings constructed after 2015 must comply with these building energy conservation measures. For the envelope design, GB 50189-2015 also regulated an envelope trade-off compliance path, allowing thermal transmittance of some envelopes exceeding its prescriptive limit if the proposed building's overall energy use with the integrated design is not higher than the code-compliant baseline building. This path can be achieved by applying cool envelopes or improving the thermal performance of other components of the building [29]. The trade-off option offers more flexibility for thermal design, balancing the buildings' thermal and energy performance [30]. Therefore, the potential benefits of cool-coated buildings at the design stage can be achieved in two ways: (1) initial cost savings by reducing insulation material thickness without exceeding the building's allowed energy use intensity, or (2) energy cost savings by reducing the solar heat gain conducted through the envelope assembly based on optimization of envelope albedo and insulation. The benefits mentioned above necessitate the design optimization of cool-coated buildings based on envelope trade-off compliance calculations to achieve minimal life-cycle costs.

1.2 Novelty and main contributions

This study proposes a holistic approach integrating field testing, building energy simulation, and a 20-year life-cycle-based optimization to explore the maximum potential benefit of cool-coated buildings and the maximum net savings achieved by optimal retrofit and design of building envelope. An experiment was conducted in a three-story office building located in Chongqing, a city in China's hot summer and cold winter climate zone (Appendix A Fig. A-1), to investigate thermal performance improvement when applying cool walls. A building model was developed based on the tested building by EnergyPlus and was validated using the experimental data. Both retrofit and design optimization for building envelope was conducted to achieve the maximum net savings.

The original contributions of this study are briefly summarized as follows: (1) The potential benefits of cool-coated buildings (combined use of cool roofs and walls) were comprehensively investigated. (2) Both the envelope design and retrofit optimization were comprehensively conducted, which provides promising alternatives for designers and engineers to make their best decisions based on quantitative assessment.

2 Methodology

2.1 Overview and procedure

A systematic and generic approach is proposed to evaluate cool envelopes' performance and conduct both retrofit and design optimization for cool-coated buildings based on life cycle cost analysis, as shown in Fig. 1. In the first step (panel a), two test rooms' thermal and energy performance were evaluated in a three-story office building, and the results were used to validate the building model developed using EnergyPlus [31]. Here, the thermal performance of the test rooms was evaluated by measuring the differential surface temperature with and without applying cool coatings. The energy performance of the test rooms was evaluated by measuring the differential air-conditioning energy use with and without applying cool coatings. In the second step (panel b), two building prototypes, namely "old building" (with high thermal transmittance) and "new building" (with low thermal transmittance), were developed based on the validated building model. In the third step (panel c), building energy simulations were conducted to investigate the maximum potential benefits of cool-coated old and cool-coated new buildings. In the fourth step (panel d), the building envelope albedos and or insulation thickness were optimized for the retrofit case and design case, respectively, to achieve a minimal life cycle cost. The optimization procedure was enabled by coupling MATLAB with EnergyPlus, which is further described in Section 2.4.

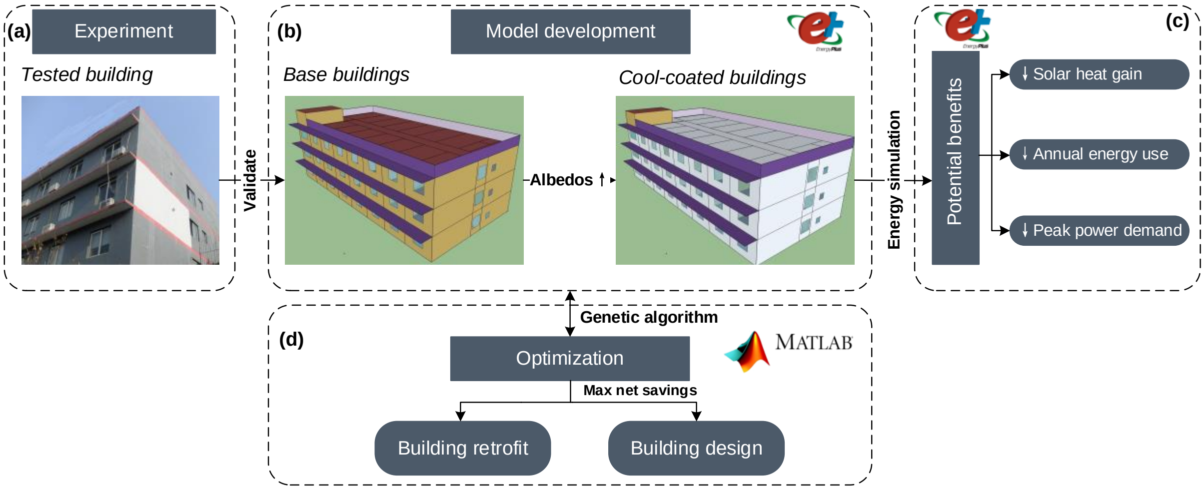

Fig. 1. Process and steps of the proposed approach.

2.2 Experimental study

On Aug 14 – 28, 2013, the experiment was conducted in a three-story office building in Chongqing, China. The cool wall of room 214 (the base approximately 7 m from the ground) and gray wall of room 314 (the base of the wall approximately 10 m from the ground) on the second floor and the third floor, respectively, to the west, are shown in Fig. 2. The cool wall was painted with a highly reflective coating (initial albedo 0.84), while the gray wall had a low albedo around 0.2. Here, the initial albedo of cool coatings was derived from the performance test report provided by the coating manufacturer, which was measured by the Natural Research Center of Testing Techniques for Building Materials following the Chinese standard GB/T9755-2001 *Synthetic resin emulsion coatings for exterior wall* [32]. As the coatings were painted on the west wall in July 2013 and we conducted the experimental test subsequently in Aug 2013, the cool coating aging and albedo degradations were ignorable. The initial gray wall surface was covered by the latex paint. Although the albedo of the initial gray wall could not be measured as no samples were available, the color and composition lead us to consider a value of 0.2 [33].

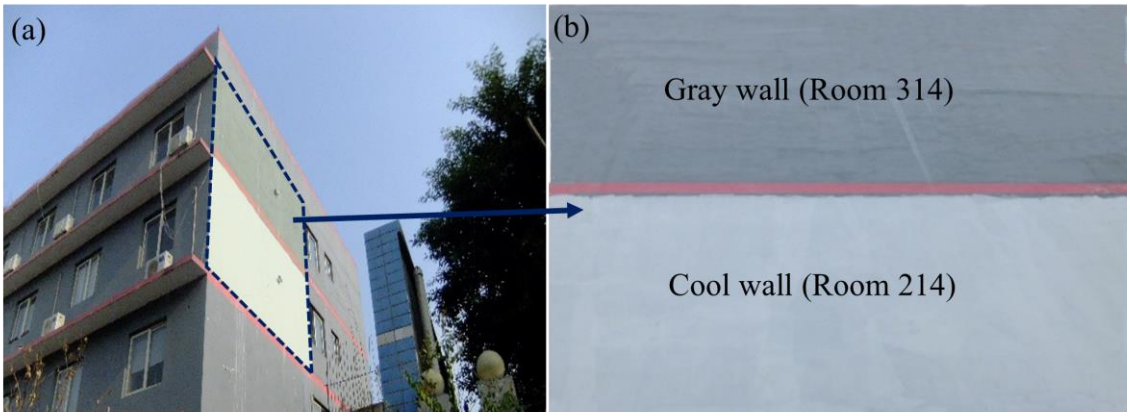

Fig. 2. Views of (a) the tested building and (b) its west wall.

Table 1. Main features of the test building.

General information	
Location	Jiangjin District, Chongqing city, China
Latitude and longitude	29.35°N, 106.43°E
Elevation above sea level (m)	209
Building type	Office building
Main orientation	North-South
Building shape coefficient (surface-to-volume ratio) (m^{-1})	0.23
Window-to-wall ratio	0.17 (north and south), 0.06 (west), 0.19 (east)
Building envelope	
Walls	Three layers (outside to inside: 20 mm anti-crack layer, 230 mm clay hollow brick, and 20 mm cement mortar) with total thermal transmittance of 2.10 $W/m^2 \cdot K$
Roof	Three layers (outside to inside: 5 mm waterproof layer, 20 mm cement layer, 100 mm reinforced concrete) with total thermal transmittance of 4.10 $W/m^2 \cdot K$
Floor	Four layers (outside to inside: 20 mm cement mortar, 30 mm extruded polystyrene board, 100 mm reinforced concrete, 20 mm cement mortar) with total thermal transmittance of 0.85 $W/m^2 \cdot K$
Windows	Double glazing (outside to inside: 5 mm glass, 5 mm air, and 5 mm glass), an unplasticized polyvinyl chloride window frame, with total thermal transmittance of 3.20 $W/m^2 \cdot K$
Specifications of air conditioners (ACs)	
Make and model	Model 1 for Room 214: Midea, KFR-26GW/DY-GC(R3) Model 2 for Room 314: Midea, KFR-35GW/DY-IA(R3)
Rated coefficient of performance (COP) (W/W)	Model 1: 3.28 for cooling and 3.75 for heating Model 2: 3.28 for cooling and 3.67 for heating
Rated capacity (kW)	Model 1: 2.6 kW cooling and 3.0 kW for heating Model 2: 3.5 kW cooling and 4.0 kW for heating
Setpoint (°C)	26 °C for cooling and 20°C for heating
Operating schedule	00:00 – 24:00

Table 2 and Fig. 3 give the specification of instruments and the locations of the sensors, respectively. The monitored rooms were equipped with data acquisition systems that connected all surface temperature (excluding the rooftop) sensors and recorded the measured data at a 1-min interval. A handheld infrared thermometer and a handheld pyranometer were used to measure rooftop surface temperature and horizontal global solar irradiance, respectively, at a 1-

hour interval from 7:00 to 24:00 local standard time (LST). A thermal imaging camera was used to capture the whole surface temperature of cool and gray walls at a 1-hour interval from 7:00 to 19:00 LST. Air-conditioner electricity uses of rooms 214 and 314 were recorded by smart power meters. As the upper room 314 received heat from the roof while the lower room 214 did not, the estimation of cool wall energy savings based on measurements becomes complicated. Instead, such energy savings were evaluated based on simulation analysis.

Table 2 Measurement sensors and protocols.

Measurement	Details
Exterior and interior surface temperature of the west wall and ceiling surface temperature (Room 214 and 314)	
Sensor type	Resistance thermometer PT1000
Sensor range	-20 to +150 °C
Sensor accuracy	±0.2 °C
Protocol	Sensor attached on the surface; measurements logged internally every 1 min
Indoor air temperature (Room 214 and 314) and ambient temperature	
Sensor type	Temperature micrologger
Sensor make & model	China Academy of Building Research Co., Ltd. (RR002)
Sensor range	-10 to +50 °C
Sensor accuracy	±0.5 °C
Protocol	Sensor suspended 1.5m above floor or ground; measurements logged internally every 1 min
Rooftop surface temperature	
Sensor type	Handheld infrared thermometer
Sensor make & model	Raytek ST
Sensor range	-32 to +535°C
Sensor accuracy	±1 °C
Protocol	Instrument held 1.5 m from the rooftop; hourly measurements recorded manually from 07:00-24:00 local standard time
Global horizontal solar irradiance	
Sensor type	Handheld pyranometer
Sensor make & model	Jinzhou Sunshine Technology Co., Ltd. (TBQ-2)
Sensor range	0 to 2,000 $W \cdot m^{-2}$
Sensor accuracy	±2%
Protocol	Instrument held 1.5 m from the rooftop; hourly measurements recorded manually
Exterior surface temperature distribution of the west wall (Room 214 and 314)	
Sensor type	Thermal imaging camera
Sensor make & model	FLIR Systems, Inc. (ThermaCAM P30)
Sensor range	-40 to +1,000℃
Sensor accuracy	±2 °C
Protocol	Instrument held 2.0 m from the wall; hourly measurements recorded manually

Air-conditioner electricity use (Room 214 and 314)	
Sensor type	Smart power meter
Sensor make & model	Shenzhen northmeter Co., Ltd. (Power Bay-SSM)
Sensor accuracy	±1%

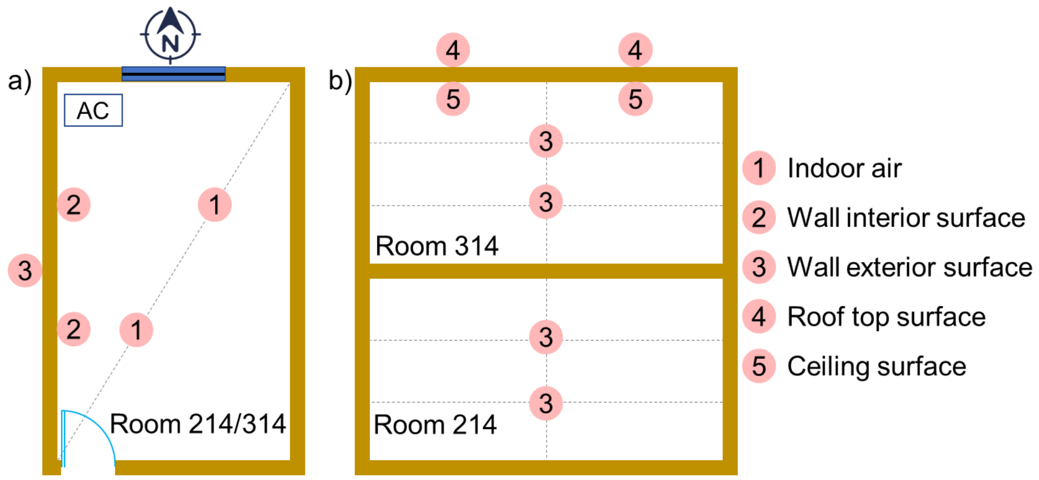

Fig. 3. Temperature sensor locations in (a) top view and (b) side view.

2.3 Simulation analysis

2.3.1 Model validation

Before conducting the building energy simulation analysis, a building was developed to mimic the tested building by EnergyPlus and was validated by the experimental data. The building model (Fig. 4a) had the same construction, layout, dimension, temperature setpoints, internal load (occupancy, lighting, and equipment) as the tested building. The packaged terminal heat pump model was selected and set with the same rated COP and rated capacity as the real ACs. The ACs in the building model operated based on indoor and outdoor environmental conditions [34][35]. The hourly on-site measured meteorological data (e.g., global horizontal solar irradiance and outdoor dry-bulb temperature) were also used as weather inputs for model validation. The layout of the top floor (containing 14 rooms) in the building model is shown in Fig. 4b. The measured data from 14 to 28 Aug were used to validate the building model. (1) The thermal performance of the building envelope was validated by comparing the simulated and measured exterior and interior roof/wall surface temperatures. (2) The cooling performance of the air-conditioners was validated by comparing the simulated and measured AC electricity consumption.

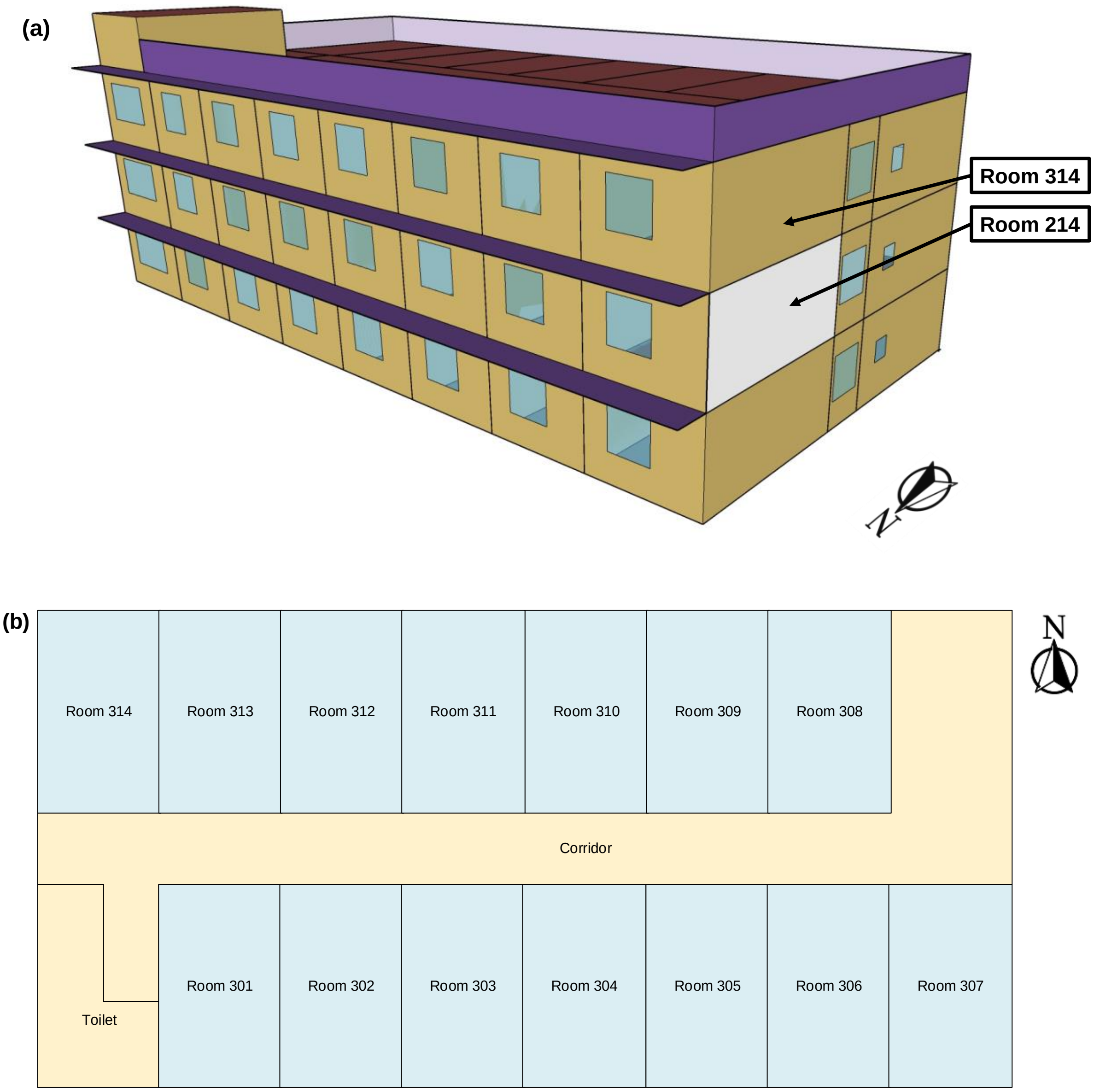

Fig. 4. (a) 3-D rendering of the building simulation model and (b) layout of the building model's top floor.

Several indicators commonly used for validating building performance simulation models [36] were adopted in this study. The mean absolute error (MAE), mean bias error (MBE), and coefficient of variation of root mean square error CV(RMSE) were computed using Eqs. (1)-(3), respectively.

$$\mathrm{MAE} = \frac{1}{N_p}\sum_{i=1}^{N_p}(r_i - q_i) \tag{1}$$

$$\text{MBE } (\%) = \frac{\sum_{i=1}^{N_p}(r_i - q_i)}{\sum_{i=1}^{N_p}(r_i)} \quad (2)$$

$$\text{CV(RMSE) } (\%) = \frac{\sqrt{\sum_{i=1}^{N_p}(r_i - q_i)^2 / N_p}}{\bar{r}} \quad (3)$$

where r_i and q_i are the measured and simulated data points for each model instance i, respectively. N_p is the number of data points at interval p (i.e., $N_{\text{monthly}} = 12$, $N_{\text{hourly}} = 8{,}760$). $\bar{r}$ is the average of the measured data points. In this study, the accuracy of the building model's surface temperature was assessed using the MAE. The accuracy of AC electricity use of the present building model was assessed using the hourly criteria in ASHRAE Guideline 14 [37], in which the MBE and CV (RMSE) should be lower than 10% and 30%, respectively.

2.3.2 Quantification of potential benefits of cool-coated buildings

Cool-coated buildings can save the building energy use and energy cost, as well as reduce the peak power demand. Two building prototypes, namely "old building" and "new building", were developed for evaluating the potential benefits of cool-coated buildings by the building energy simulation using EnergyPlus.

The old building prototype was developed by updating the validated building models (in Section 2.3.1) with the following settings: (1) the roof albedo and wall albedo were set to 0.20 and 0.25, respectively, representing the gray roof and gray wall [12]; (2) typical meteorological year (TMY3) data [38] of Chongqing Shapingba 575160 (CSWD) were used as the weather inputs; and (3) all rooms were equipped with the validated AC model of test room 314. The construction of the "old building" prototype is the same as the test building listed in Table 1.

The new building prototype was developed by further updating the old building prototype with well-insulated construction (i.e., low thermal transmittance), following the prescriptive requirements of the new Chinese building design standard GB 50189-2015 [27]. Table 3 shows the new building prototype's envelope construction, thermal transmittance, and the prescribed maximum thermal transmittance.

Table 3 Roof and exterior wall construction (listed from outside to inside).

Envelope type	Construction (outside to inside)	Thermal transmittance (W/m^2·K)	Prescribed maximum thermal transmittance (W/m^2·K)
Roof	4 mm waterproof layer + 20 mm cement mortar + 60 mm expanded polystyrene (EPS) + 55 mm cement expanded perlite + 100 mm reinforced concrete + 20 mm cement	0.48	0.50

	mortar		
Exterior wall	5 mm anti-crack mortar + 30 mm EPS + 240 mm hollow brick walls with porous clay bricks + 20 mm cement mortar	0.76	0.80

The entire office building was used as the simulation object. For both the prototypes, the design values and daily patterns for occupant density, lighting load, equipment load, and minimum fresh air supply were set following GB 50189-2015 [27], as presented in Table 4 and Fig. 5, respectively. The heating and cooling setbacks are 5°C and 37 °C, respectively, to avoid the indoor air temperature in unoccupied periods being too hot in summer or too cold in winter. We assumed that no person or building service systems worked on weekends.

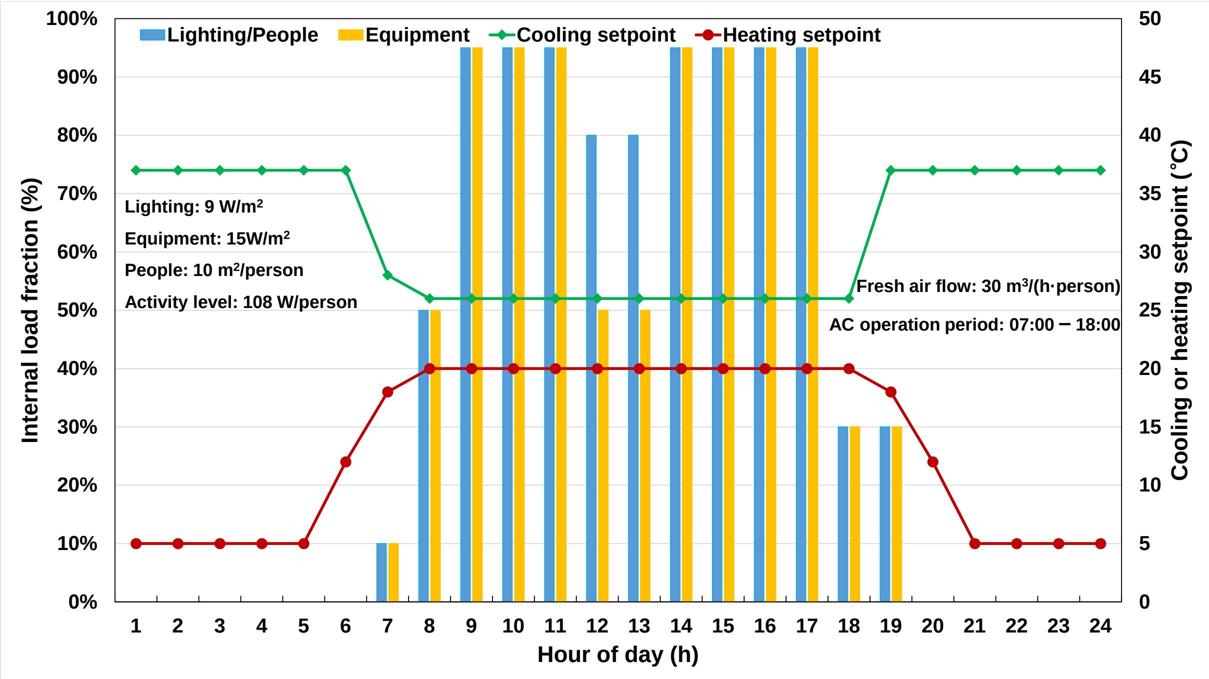

Fig. 5. Daily air-conditioning hourly temperature setpoints, internal load (occupancy, lighting, and equipment) hourly schedule in a typical office building on weekdays.

Table 4 Design values of occupant density, lighting load, equipment load, minimum fresh air supply, and AC operation hours.

Occupant density (m^2/person)	Lighting (W/m^2)	Electrical equipment (W/m^2)	Fresh air supply (m^3/h/person)	AC operation hours
10	9	15	30	07:00 – 18:00

The performances of old and new base buildings were evaluated through energy simulation based on the created old and new building prototypes, respectively. The potential benefits of cool-coated old and new buildings were quantified by further raising only the albedos of the prototypes without changing other parameters. The roof albedo and wall albedo of cool-coated buildings were each set to 0.60, representing aged cool roofs and aged cool walls [12][39].

2.4 Optimization methods

2.4.1 Optimization framework

Fig. 6 shows the proposed optimization framework in this study. The first step involved the development of the building models by EnergyPlus. In the building energy simulation, EnergyPlus typically uses text-based inputs, such as Input Data File (IDF) files, and outputs the simulation results in comma-separated value (CSV) text files. In the second step, a coupling engine developed in a platform (i.e., MATLAB) supporting optimization algorithms loaded the IDF file as a data structure and tuned the IDF file parameters based on the values of the problem's decision variables in each iteration. The coupling engine then sent the IDF file back to EnergyPlus for simulation and got the simulation results from the EnergyPlus output (CSV) file to evaluate the objective functions. To accelerate the optimization, the Parallel Computing Toolbox™ [40] in MATLAB was used to distribute the tasks in parallel rather than in serial. In the third step, the genetic algorithm (GA) [41] from the Global Optimization Toolbox™ in MATLAB was implemented to obtain the optimal solutions. The process was repeated until the GA converges to output the unique optimal solution for the problem objectives.

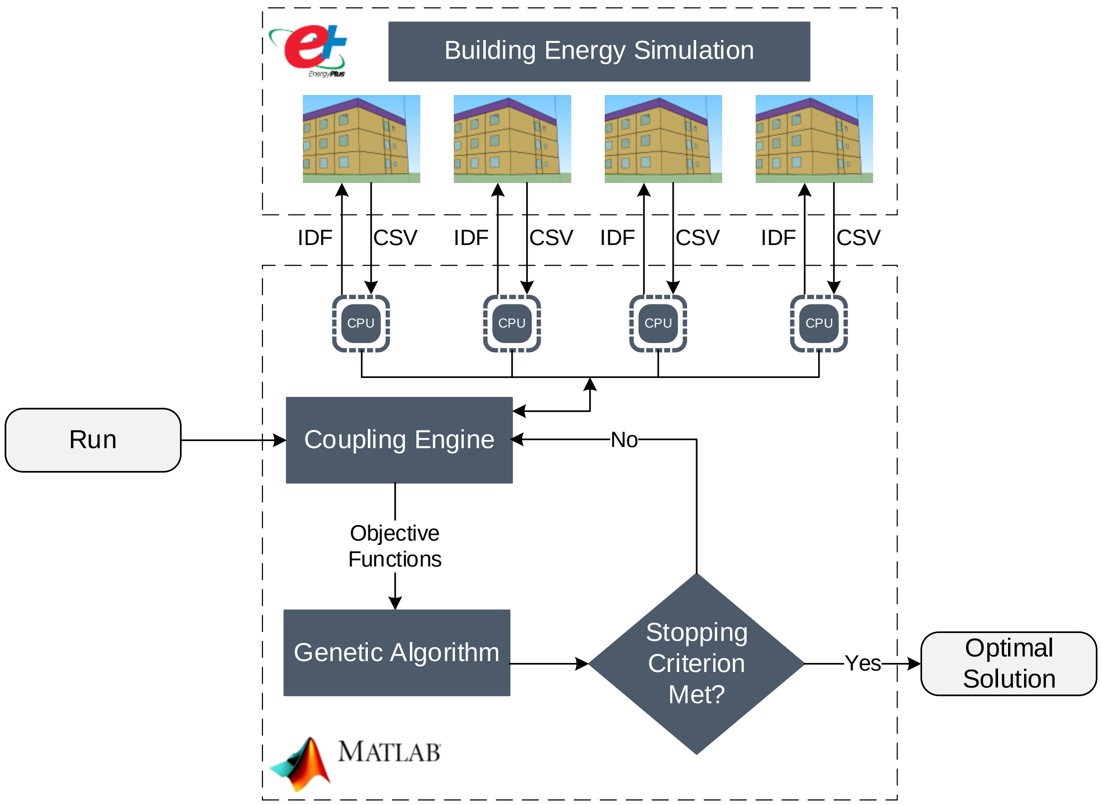

Fig. 6. Proposed optimization framework.

2.4.2 Research cases and decision variables

Two types of research cases: (1) building envelope retrofit and (2) building envelope design, were performed in the optimization procedure by modifying decision variables. Table 5 shows the research cases and their decision variables. The decision variables represent the set of alternative measures allowing for the corresponding research case optimization. All decision variables were set continuously to provide more granularity in the optimization and broaden the problem's search space.

The building envelope retrofit optimization (for existing buildings) was conducted based on both old and new building prototypes by modifying the envelope albedos only. The albedos of all five envelope surfaces (four walls + a roof) were optimized. The lower bound and upper bound of wall albedos were set as 0.25 and 0.60, respectively [12][39], while the range of the roof albedo was between 0.20 and 0.60 [17]. The albedos of four walls and a roof were optimized independently. The building envelope design optimization (for buildings to be designed or having not been constructed yet) was conducted based on the new building prototype by modifying the (1) insulation, (2) albedo, and (3) both albedo and insulation of envelopes. The optimally designed buildings should meet the current 2015 building code's trade-off compliance path, in which the thermal transmittances of some components can exceed their prescribed higher limits.

Table 5 Research cases and decision variables.

Research cases	Building prototype	Decision variable	
		Description	**Range**
Building retrofit	Old building	Wall albedo (-)	0.25 – 0.60
		Roof albedo (-)	0.20 – 0.60
	New building	Wall albedo (-)	0.25 – 0.60
		Roof albedo (-)	0.20 – 0.60
Building design	New building	Wall EPS insulation thickness (mm)	0 – 60
		Roof EPS insulation thickness (mm)	0 – 120
	New building	Wall albedo (-)	0.25 – 0.60
		Roof albedo (-)	0.20 – 0.60
	New building	Wall albedo (-)	0.25 – 0.60
		Roof albedo (-)	0.20 – 0.60
		Wall EPS insulation thickness (mm)	0 – 60
		Roof EPS insulation thickness (mm)	0 –120

2.4.3 Objective functions and problems formulation

The objective of building envelope retrofit/design optimization is to maximize the present value of net savings (Y) of the building envelope retrofit/design by minimizing its additive inverse (Eq. (4)):

$$min \quad -Y \tag{4}$$

Eq. (5) calculates the net savings:

$$Y = \sum_{z=0}^{N} \frac{\Delta S_{x,z} e_z}{(1+r)^z} - \sum_{t=0}^{N} \frac{\Delta C_{x,z}(1+e_c)^Z}{(1+r)^z} \tag{5}$$

where $\Delta S_{x,z,}$ and $\Delta C_{x,z}$ represents the savings and cost difference for research case x in year z between the optimized building and base building, respectively. The subscript x refers to the research cases in Table 5. r is the intergenerational real discount rate (set to 3%), and e_z and e_c are the average compounded annual electricity price escalation rate factor (ranging from 0.96 – 1.02) in year z for the commercial end-use sector and annual escalation rates for costs (averaging 0.4–2.6%) [42], respectively. N is the number of years in the life cycle (20 years [17][18]). A positive net savings indicates that the optimized building is more cost-effective than the base building.

Savings ($\Delta S_{x,z}$): In this study, $\Delta S_{x,z}$ for both building envelope retrofit and design equals the HVAC electricity cost savings, calculated by multiplying the γ_e by the annual HVAC electricity savings. The fixed electricity price (γ_e = 0.781 CNY/kWh) was adopted to calculate the electricity cost for the commercial customer [43].

Cost difference ($\Delta C_{x,z}$): $\Delta C_{x,z}$ includes the maintenance cost difference and the initial cost difference. This study treated the maintenance costs of both cool and non-cool envelopes, as well as the initial costs of both cool and non-cool coatings, as identical. The reasons are listed as follows: (1) Non-cool and cool surfaces have similar maintenance procedures, including the repair of punctures, splits, leaks, etc. According to a report by Levinson et al. [39], "cool" products can maintain their high albedo upon natural exposure. In this study, we assumed brand new cool surfaces are weathered with a stabilized albedo of only 0.60. Thus, the annual maintenance costs for non-cool and cool surfaces were set the same. (2) In terms of the initial costs between the cool and non-cool coatings, a guideline released by the U.S. Department of Energy [44] shows that cool surface products are usually similar in cost or slightly more expensive than similar non-cool alternatives. For instance, the median market price of a white single-ply membrane is the same as a black single-ply membrane. A study by Sproul et al. [17] also set the first installation costs of the cool and black roofs to be the same at 22 USD/m^2. Thus, the initial costs for cool and non-cool coatings were set to be identical.

For building envelope retrofit, as there is no opportunity to reduce material and labor expenses using less insulation, the cost difference $\Delta C_{x,z}$ only includes the coating initial cost difference (ΔC_{coat}). For building envelope design, as the market prices of cool coatings and common gray coating are identical, the cool-surface cost premium can be regarded as zero at the design stage. Therefore, the cost difference $\Delta C_{x,t}$ only involves its initial cost difference of EPS material (ΔC_{EPS}). $\Delta C_{x,z}$ for different research cases, is presented in Eq. (6**Error! Reference source not found.**).

$$\Delta C_{x,z} = \begin{cases} \Delta C_{coat}, & \text{for envelope retrofit} \\ \Delta C_{EPS}, & \text{for envelope design} \end{cases} \tag{6}$$

According to the rated criteria for cool roof products by ENERGY STAR [45], cool materials must have an initial albedo greater than or equal to 0.65 and an aged albedo greater than or equal to 0.50. Therefore, in this study, a coated surface with aged albedo greater than or equal to 0.50 is regarded as a cool surface, while a coated surface with aged albedo lower than 0.50 is regarded as a non-cool surface. The coating initial cost difference ΔC_{coat} can be calculated by Eq. (7), where i refers to the envelope of the building (i.e., 1 to 4 represents four walls respectively, and 5 represents the roof). A_i is the envelope area. ρ_i refers to the envelope albedo, and K_i is the indicator for coated envelopes calculated by Eq. (8). The capital cost of coatings

(γ_{coat}) includes the capital cost and the labor cost for coating, 38.7 CNY/m^2 in Chongqing [18]. For instance, selecting an aged roof albedo of 0.2 indicates retrofit work for the roof is not required. Selecting an aged roof albedo in the range of (0.2, 0.5) indicates the roof should be painted with non-cool coatings. Selecting an aged roof albedo in the range of [0.5, 0.6] indicates the roof should be painted with cool coatings. It is worth noticing that we assumed that retrofitting the envelope covering can be conducted before the end of its service life to offer more flexibility for the decision-makers. Therefore, the decision-makers can determine whether to adopt the cool coatings at any service time of envelope.

$$\Delta C_{coat} = \sum_{i=1}^{5} \gamma_{coat} A_i K_i \tag{7}$$

$$K_i = \begin{cases} 1, & \rho_i > 0.25 \text{ (i = 1 to 4)} \\ 0, & \rho_i = 0.25 \text{ (i = 1 to 4)} \\ 1, & \rho_i > 0.2 \text{ (i = 5)} \\ 1, & \rho_i = 0.2 \text{ (i = 5)} \end{cases} \tag{8}$$

Eq. (9) calculates the EPS initial cost difference ΔC_{EPS}. Here, $d_{o,i}$ represents the optimal insulation thickness for i^{th} envelope and $d_{b,i}$ represents the original insulation thickness of base buildings for i^{th} envelope. The EPS insulation price (γ_{EPS}, CNY/m^2) under different thicknesses (d>0 mm) was evaluated using Eq. (10) [46], taking account of both the material and installation costs (i.e., assumed as 30% of the material cost [47]).

$$\Delta C_{EPS} = \sum_{i=1}^{5} \gamma_{EPS} \left(d_{o,i} - d_{b,i}\right) A_i \tag{9}$$

$$\gamma_{EPS} = 1{,}220d + 69.5 \tag{10}$$

2.4.4 Genetic algorithm settings

The GA algorithm operates on a finite set of simulations (population). At each step, the GA randomly selects individuals from the current population and lets them compete to select the best one that fits the objective. Over successive generations, the population "evolves" toward an optimal solution. According to the Global Optimization Toolbox™ [48], the population size should be set based on the variable number. When the number is less than or equal to 5, the population size should be 50. Otherwise, the population size should be 200. Table 6 shows the related settings for GA.

Table 6 Population size, maximum generations for GA.

Research cases	Building type	Variable type	Variable number	Population size	Maximum generations
Building retrofit	Old building	Albedo	5	50	50
	New building	Albedo	5	50	50
Building design	New building	Insulation	5	50	50
	New building	Albedo+Insulation	10	200	50

3 Results

3.1 Experimental and model validation results

3.1.1 Weather conditions

From 14 Aug to 28 Aug 2013, 15 summer days were selected as representative days to test the thermal performance of cool coatings and validate the prototype building model. Most of the days were sunny during the test period. Fig. 7 shows the solar radiation and outdoor air temperature on the test days. It can be seen that the outdoor air temperature oscillated between 25.1 °C and 43.2 °C, and the maximum daily value of global horizontal solar irradiance varied between 273 W/m^2 and 1,180 W/m^2.

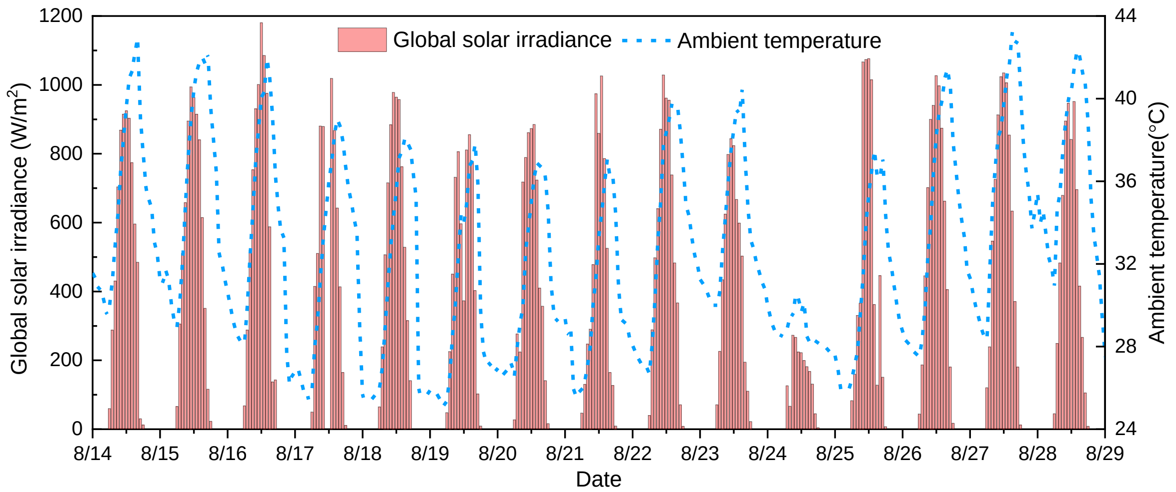

Fig. 7. Global horizontal solar irradiance and outdoor air temperature.

3.1.2 Thermal performance of cool wall and model validation results

Fig. 8 shows the measured data of the monitored rooms, including the exterior and interior surface temperatures of the west walls (a gray wall and a cool wall), exterior and interior surface temperature of the roof, and the hourly AC electricity use. As the upper room 314 received heat from the roof while the lower room 214 did not, affecting the indoor environment or AC electricity use, only the exterior and interior surface temperature profiles of the west walls were used to demonstrate cool walls' cooling effects. During the test period, the gray wall's exterior surface temperature peaked at 56.7 °C (17:00, Aug 27), while the cool wall peaked at 50.7 °C (16:00, Aug 27). The cool wall was up to 9.3 °C cooler than the gray wall occurring at 17:00, Aug 17. It is worth noticing that, some electricity use data were missing due to the intermittent power outage and packet loss.

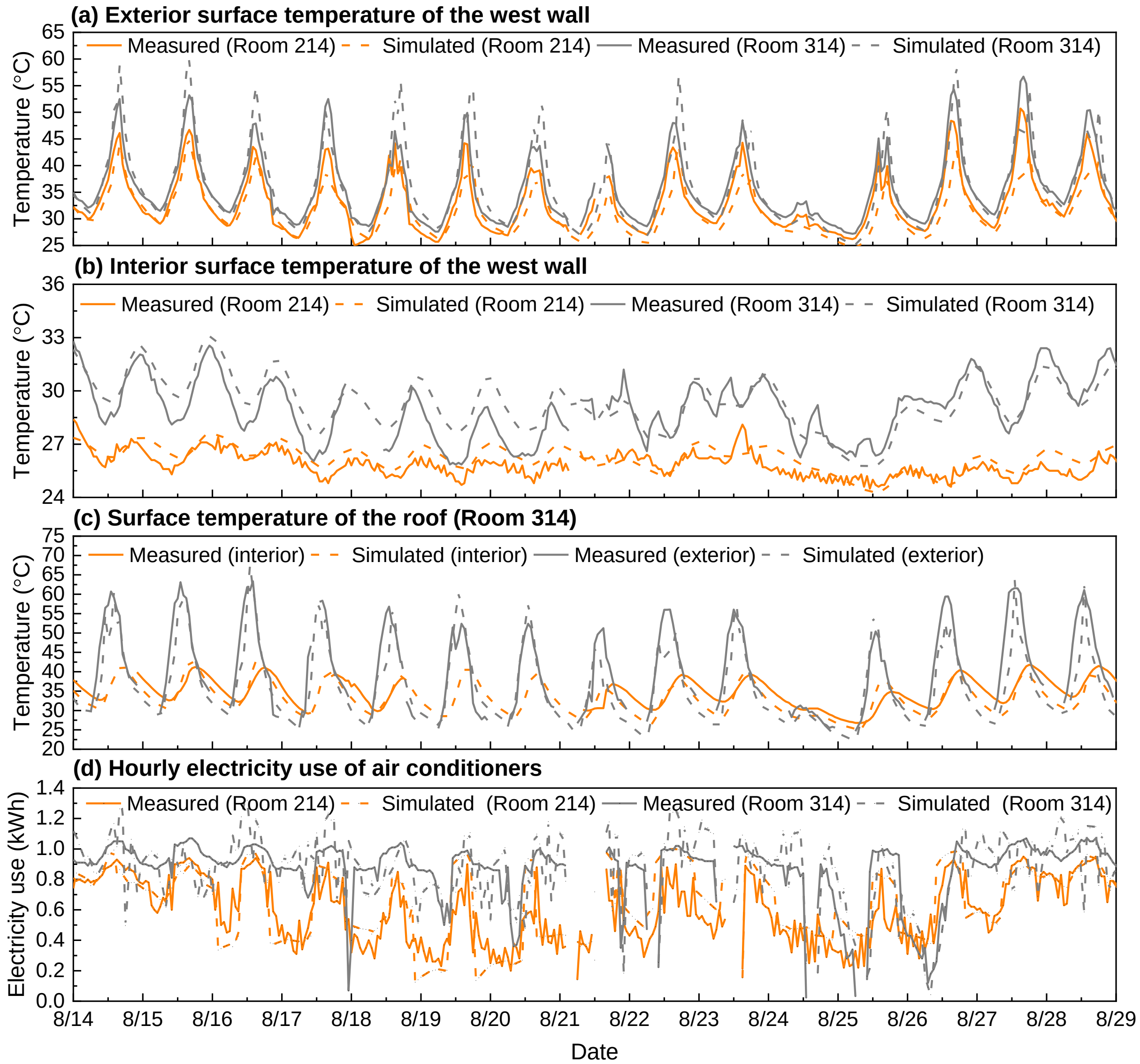

Fig. 8. Comparison between experimental and simulation results in the test building, showing (a) exterior surface temperature of the west walls, (b) interior surface temperature of the west walls, (c) surface temperature of the roof over room 314, and (d) hourly electricity use of air conditioners.

Thermal images provide fast temperature measurements in the whole cool and gray walls.

Although radiometric temperature measurements are not as accurate as contact temperature measurements, they can help identify uneven painting. The cooling effects of the cool wall can also be observed intuitively. Fig. 9 shows the exterior surface temperature distributions of cool and gray walls at 13:53 LST on 17 Aug. The distinct boundary (yellow and green area) in the middle of the panel (a) of Fig. 9 is due to the impacts of pink painting (used to divide the cool and gray walls) and the conductive heat transfer between the walls. The average temperature of the cool wall was 5.6 °C lower than that of the gray wall. The temperature range was 32.9 – 35.3 °C for the cool wall and 38.0 – 40.7 °C for the gray wall. The temperature deviations among the same area (gray wall area or cool wall area) were mainly due to the irregularities or unevenness of coatings.

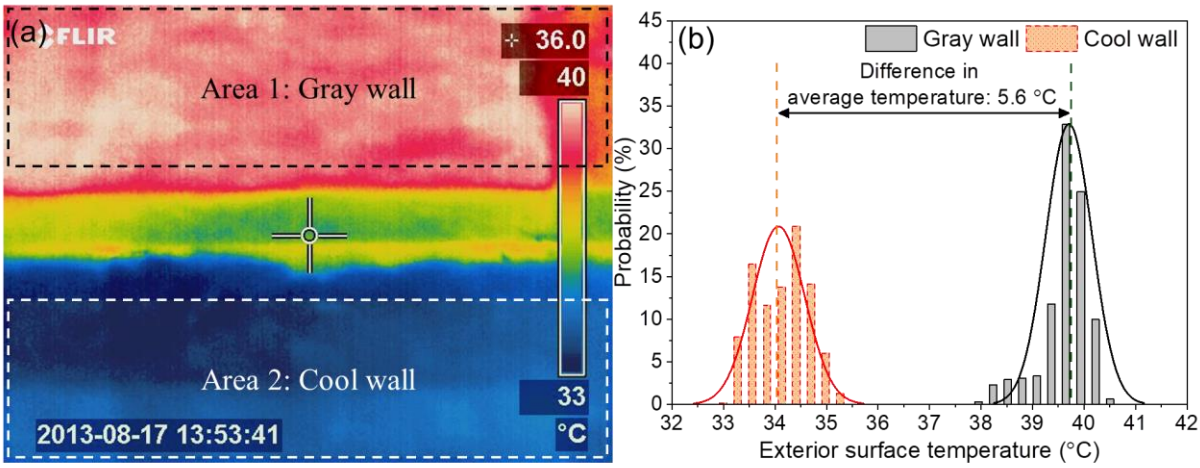

Fig. 9. Exterior surface temperature comparison between cool and gray walls (a) infrared image (b) temperature distribution at 13:53 LST on 17 Aug.

Fig. 8 also shows the difference between the measured and simulated data. Actually, for the validation of the building model, the model inputs (i.e., weather, occupancy, lighting and electric appliances) were set following the actual conditions during the experimental period. Here, the actual weather conditions used for model validation are presented in Fig. 7. During the office hours (07:00-18:00) in the test period, two test rooms (214 and 314) were mostly not occupied, and the windows/doors were fully closed. Therefore, the air infiltration and internal loads (i.e., from occupancy, lighting, and electric appliances) were set zero for model validation. The MAE, MBE, and CV(RMSE) between the measured and simulated data are calculated as listed in Table 7. The MAE between the measured and simulated temperatures varied between -2.8 and 0.6 ºC. The MBEs and CV(RMSE)s between the measured and simulated hourly electricity uses fulfilled the acceptance criteria of model validation (i.e., MBE < 10% and CV(RMSE) < 30%). This criterion indicates that the present building model was wellestablished and could be used to simulate with good reliability the daily profiles of the surface temperatures and the total daily electricity consumption of the air-conditioners of rooms.

Table 7 Model validation of prototype building.

Indicator	Exterior surface temperature of the west wall		Interior surface temperature of the west wall		Surface temperature of the roof over room 314		Hourly electricity use of air conditioners	
	Room 214	Room 314	Room 214	Room 314	Interior	Exterior	Room 214	Room 314
MAE (ºC or kWh)	-1.4	0.2	0.6	0.4	-1.7	-2.8	0.05	0.01
MBE (%)	-	-	-	-	-	-	7.9	0.8
CV (RMSE) (%)	-	-	-	-	-	-	26.5	22.8

3.2 Cool-coated building performance

3.2.1 Heat gain reduction

Fig. 10 gives the monthly solar irradiation on each envelope facet (excluding windows) of buildings in Chongqing, which was calculated by the Sky Radiance Model of EnergyPlus treating the Typical Meteorological Year 3 (TMY3) data of Chongqing Shapingba 575160 (CSWD) as weather inputs [49]. The solar irradiation on the roof was largest throughout the year, followed by the west, east, and north walls. The solar irradiation on the south wall was in-between that of the other three walls in different months. The absorbed solar radiation heat gain (SRHG) intensity on each envelope can be calculated by multiplying the facet absorptance with the corresponding solar irradiation. Table 8 shows the annual SRHG intensity on facets of different buildings. It can be seen that cool-coated buildings had up to 50% lower intensity than the base cases.

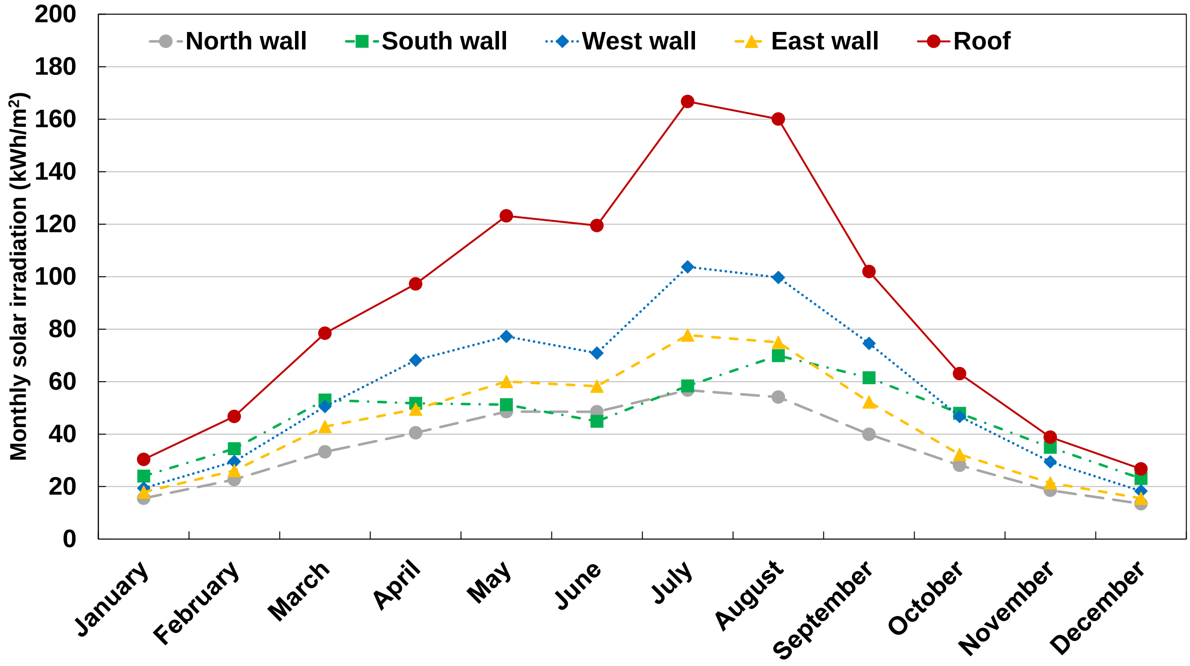

Fig. 10. Monthly solar irradiation on each envelope facet of buildings in Chongqing.

Table 8 Annual SRHG intensity on facets.

Building type	Envelope type	Base case Annual SRHG intensity (kWh/m^2)	Cool-coated case Annual SRHG intensity (kWh/m^2)	Reduction rate
Old /new buildings	North wall	227	106	46.7%
	South wall	310	145	46.7%
	West wall	376	176	46.7%
	East wall	288	135	46.7%
	Roof	607	304	50%

The room conduction heat gain (CHG) represents the amount of heat transferred to the room from the outdoor environment, which originates from a simulation output named "zone opaque surface inside faces total conduction heat gain energy". It depends on the SRHG, construction thermal transmittance, and the indoor and outdoor thermal environment. Raising the envelope albedo can reduce the SRHG, thus reducing CHG through the opaque envelope. The reduced annual CHG intensity by the cool envelope can be calculated by:

$$g = \frac{CHG_{\mathrm{b}} - CHG_{\mathrm{m}}}{A_{\mathrm{m}}} \tag{11}$$

where CHG_{b} and CHG_{m} respectively refer to the base building and to the proposed envelope modification. A_{m} is the total surface area modified. For instance, if the whole roof is coated with cool materials, A_{m} is the roof area.

Table 9 shows the reduction of annual CHG intensity of all rooms' interior surfaces caused by the corresponding cool envelope. The cool envelopes reduced about 50% annual CHG for both the old building and new building, with the reduced annual CHG intensity by 20.2 – 62.1 kWh/m^2 for the old building and 5.2 – 23.6 kWh/m^2 for the new building. The reduction of annual CHG intensity of cool envelopes in the new building was significantly lower than that of the old building due to the high insulation (low thermal transmittance) of walls and a roof in the new building. For both old and new buildings, the ranks of reduced annual CHG intensity of cool envelopes followed those of the annual SRHG intensity on envelopes (i.e., roof > west wall > south wall > east wall > north wall).

Table 9 Reduction of annual CHG intensity of buildings by cool envelopes.

Building type	Cool envelopes	Reduced annual CHG intensity (kWh/m^2)	Reduction rate
Old building	North wall	20.2	49.1%
	South wall	29.2	48.2%
	West wall	37.1	46.1%
	East wall	25.8	48.6%
	Roof	62.1	53.8%
New building	North wall	5.2	49.4%
	South wall	7.5	48.8%
	West wall	9.9	46.3%
	East wall	6.8	48.4%
	Roof	23.6	47.2%

3.2.2 Potential benefits

Electricity savings intensities by facet: When the albedo of one or more facets is modified, the annual whole-building HVAC (heating + fan + cooling), cooling, heating, and supply fan electricity savings are calculated respectively as Eq. (12), where "E" refers to the electricity use and the subscript "c" indexes the end-use. The annual electricity savings intensity j (rate per unit of modified surface area A_{m}) is then calculated from Eq. (13).

$$\mathrm{e}_c = E_{c,b} - E_{c,m} \tag{12}$$

$$j = \frac{e_c}{A_{\mathrm{m}}} \tag{13}$$

Fig. 11 shows the annual HVAC, cooling, heating, and fan electricity savings intensities of different cool envelopes in old and new buildings in Chongqing. For both old and new buildings, raising the wall or roof albedo reduced cooling and fan electricity uses but increased heating electricity use (indicated by negative savings). The sum of cooling and fan savings exceeded the heating penalty, yielding HVAC electricity savings. As the new building has better insulation, it consumed much less electricity for HVAC than the old building. Therefore, cool envelopes reduced annual HVAC electricity per unit modified surface area by 1.9 to 7.1 kWh/m^2 in the old building but only 0.9 to 1.4 kWh/m^2 in the new building. The ranking of annual HVAC electricity savings for cool facets was: roof > west wall > east wall > south wall > north wall. These rankings are slightly different from those of annual CHG intensity reduction. Although the south wall reduced more annual CHG intensity, the cool east wall saved more annual HVAC electricity than the cool south wall. The reason could be that most of the annual CHG intensity reduction provided by the cool south wall was in the heating season (e.g., November to February), resulting in significant heating penalties. The overall annual HVAC electricity savings of the cool south wall were thus reduced.

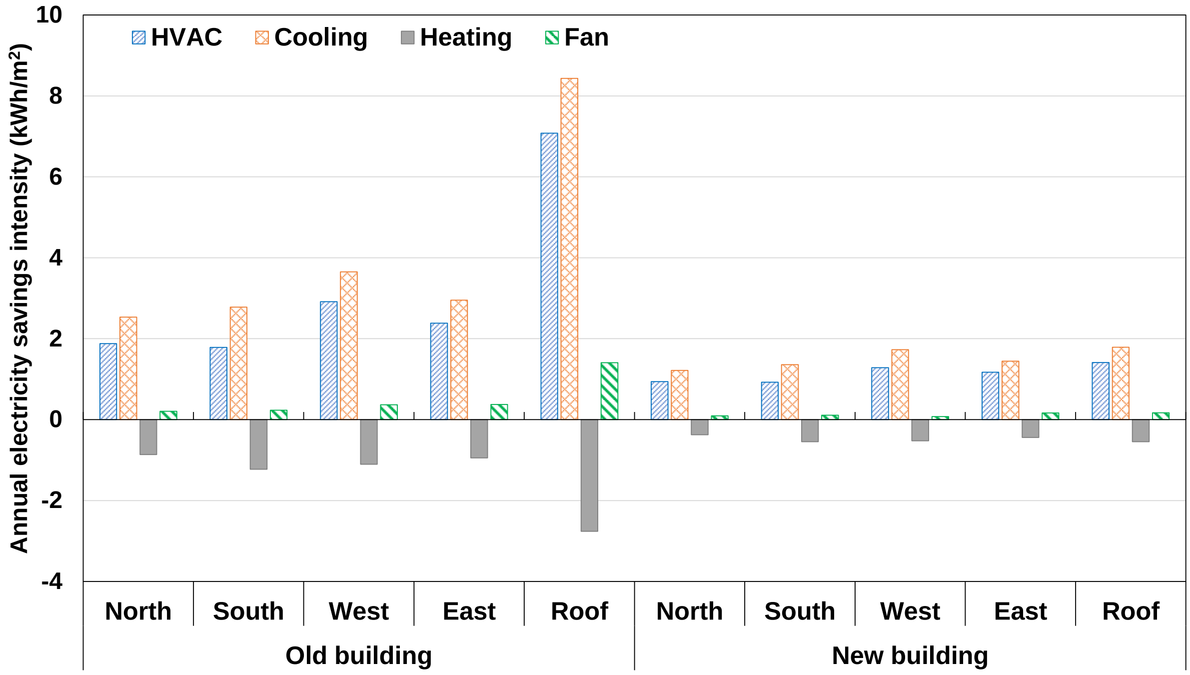

Fig. 11. Annual HVAC, cooling, heating, and fan electricity savings intensity yielded by cool facets on old and new buildings.

Electricity and cost savings of cool-coated buildings: To investigate the maximum electricity saving potentials of cool-coated buildings, all facets of existing new and old buildings were coated with cool materials. Fig. 12 shows the annual HVAC electricity use of base buildings and cool-coated buildings (with five cool facets). Cool buildings saved cooling and fan electricity but consumed more heating electricity. The cool-coated old building consumed 4.1 MWh (11.9%) less HVAC electricity each year than the old building. The cool-coated new building reduced annual HVAC electricity by 1.3 MWh (5.9%) compared with the base new building. Taking account of the total coated envelope area of 1,040 m^2, the cool-coated new building and cool-coated old building's electricity savings intensities were 3.9 kWh/m^2 and 1.2 kWh/m^2, respectively. The cool-coated old building can save 3,150 CNY/year (taking an electricity price of 0.781 CNY/kWh in Chongqing), while the cool-coated new building can save 963 CNY/year.

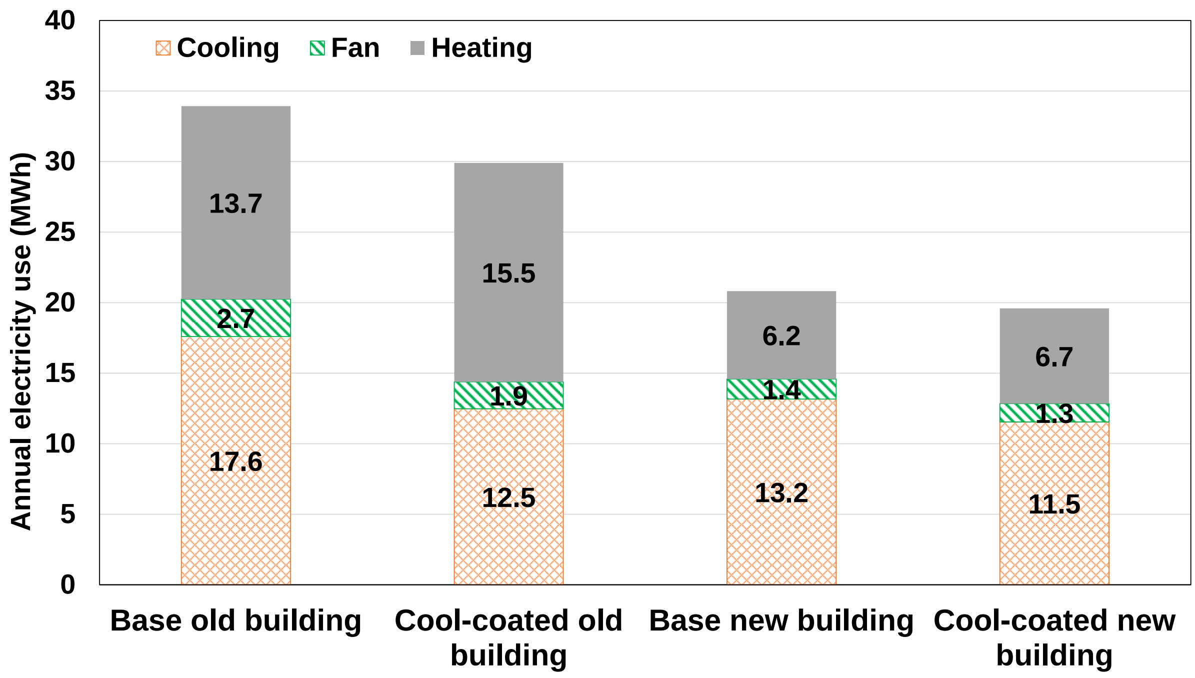

Fig. 12. Annual HVAC electricity use of four buildings.

Peak power demand savings of cool-coated buildings: Reducing the HVAC peak demand in buildings helps relieve the stress on capacities of power generation at the supply side, thus reducing the operating cost and net emission of the supply side [50]. Moreover, the reduction of HVAC peak demand can significantly reduce the electricity cost in a billing cycle for the demand side (i.e., the owner of a commercial building) if it is under a peak-demand pricing structure [51]. Although there is no additional peak demand charge in Chongqing, reducing HVAC peak demand by cool-coated buildings can be economically beneficial in other cities with the peak demand charge factor. Following Ref [12], we defined peak-demand hours between 12:00 and 18:00 on weekdays, 1 June to 1 October. Fig. 13 gives the HVAC demand power of four buildings in Chongqing on a typical summer day (8 August). During the peak-demand hours, all the demand powers went down after 12:00 due to the low internal load fraction at that time (cf. Fig. 5). They then rose after 13:00 and reached the maximum demand power at 17:00, before gradually falling at 18:00. Compared with the corresponding base building, the cool-coated old building reduces HVAC power demand by up to 8.5 kW at 18:00, and the cool-coated new building reduces HVAC power demand by up to 3.1 kW at 17:00.

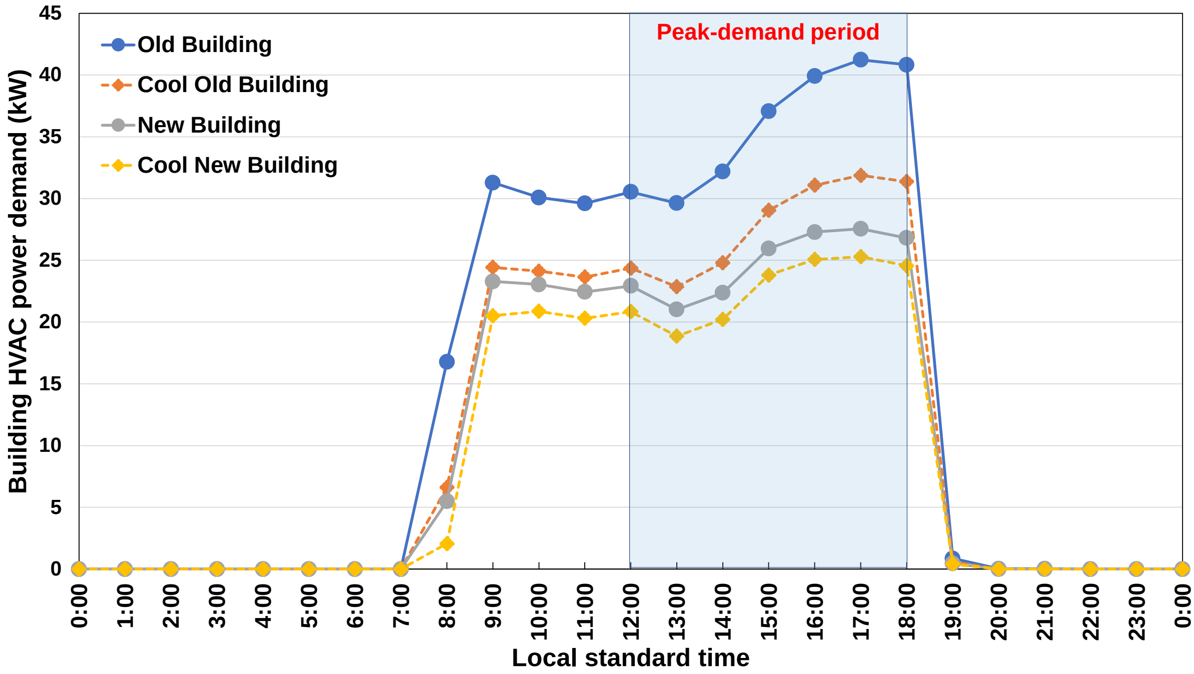

Fig. 13. HVAC power demand of four building types on a typical summer day (8 August).

The annual-average building HVAC peak-power demand reduction intensity is calculated by Eq. (14), where $e_{c,p}$ is the annual HVAC electricity savings during the peak-power period, and T is number of peak-demand hours in a year. Taking account of the total coated envelope area of 1,040 m^2, the cool-coated old building and cool-coated new building reduce the annual-average HVAC peak-power demand intensity by 2.8 kW/m^2 (24.9%) and 0.8 kW/m^2 (9.3%), respectively, as shown in Table 10.

$$w = \frac{e_{c,p}}{T \cdot A_\mathrm{m}} \tag{14}$$

Table 10 Annual-average HVAC peak-power demand reduction intensity by cool-coated buildings.

Building type	Annual-average HVAC peak-power demand reduction intensity (kW/m^2)	Reduction rate
Cool-coated old building	2.8	24.9%
Cool-coated new building	0.8	9.3%

3.3 Optimization results of building envelope retrofit and design

3.3.1 Building envelope retrofit optimization

The optimal facet albedos and the 20-year net savings for old and new buildings are shown in Table 11. For old building retrofit, it is cost-effective to apply the cool coatings (aged albedo of 0.60) only on the roof but not on walls. The net savings for the optimal old building retrofit was

1.71×10^4 CNY. Taking account of the total coated roof area of 400 m^2, the 20-year net savings per unit modified area of the coated envelope was 42.8 CNY/m^2. The optimal alternative was to avoid using cool coatings for the optimal new building retrofit, and thus the net savings was zero. It means that adopting cool coatings for retrofitting new buildings was not cost-effective since the HVAC electricity cost savings over the life cycle cannot offset the initial investment of cool coatings.

However, the research cases of building retrofit are based on the premise that the original envelopes of existing buildings are still in their service life, and thus applications of cool coatings need additional initial investments. When the original coatings on envelopes of existing buildings are at the end-of-service-life and need to be refurbished, all building envelopes are recommended to be coated with cool materials. As the initial costs (median unit prices) of cool coatings and common coatings are identical, adopting the cool coatings could offer buildings with reduced electricity costs. In this case, the net savings for the old buildings and new buildings with all five cool envelopes were 4.64×10^4 CNY and 1.42×10^4 CNY, respectively. Taking account of the total coated envelope area of 1,040 m^2, the 20-year net savings per unit area of the coated envelope for old buildings and new buildings were 44.6 CNY/m^2 and 13.6 CNY/m^2, respectively.

Table 11 Optimal facet albedos and net savings for existing buildings.

Building prototype	North wall albedo	South wall albedo	West wall albedo	East wall albedo	Roof albedo	Net savings (CNY)
Old Building	0.25	0.25	0.25	0.25	0.60	1.71×10^4
New Building	0.25	0.25	0.25	0.25	0.20	0

3.3.2 Building envelope design optimization

Optimizing the insulation thickness only: Fig. 14 gives the optimal EPS insulation thickness and net savings for the new building insulation design. The text and the value in the parentheses marked with red and green color represent the added (positive value) and reduced (negative value) EPS thickness compared to the base new building. The area covered by the solid red line with EPS pattern fill means the added EPS, while the area covered with the blue dot line with white solid fill represents the reduced EPS. The optimal solution (i.e., maximum net savings of 3,940 CNY) is EPS with different thicknesses removed from the original envelopes, except for the west wall (3.8 mm EPS added). The EPS in the roof was reduced most, followed by the south, north, and east walls.

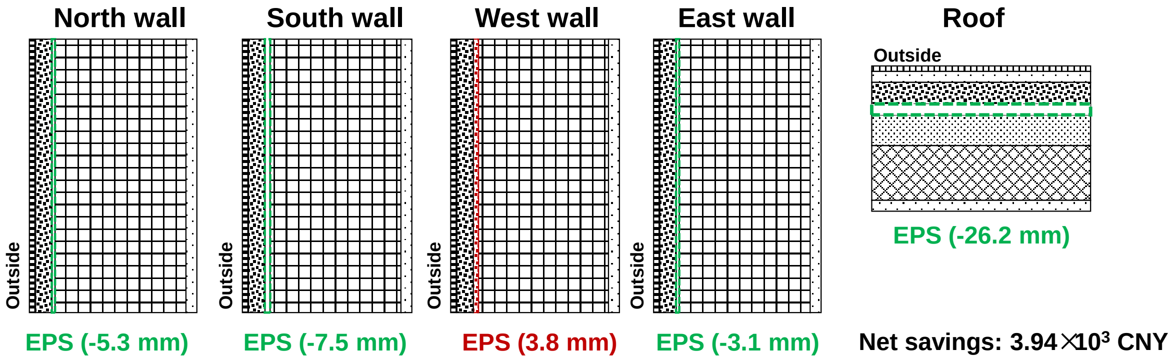

Fig. 14. Optimal EPS thickness and net savings for the new building by optimizing the insulation only.

Optimizing the albedo only: Table 12 shows the optimal envelope albedos and the 20-year net savings for the optimally designed building. Applying coatings on all building envelopes achieved a net savings of 1.42×10^4 CNY. Taking account of the total coated envelope area of 1,040 m^2, the coated envelope's net savings per unit area was 13.7 CNY/m^2.

Table 12 Optimal envelope albedos and net savings of new buildings by optimizing the albedos only.

Building prototype	North wall albedo	South wall albedo	West wall albedo	East wall albedo	Roof albedo	Net savings (CNY)
New buiding	0.60	0.60	0.60	0.60	0.60	1.42×10^4

Optimizing both the albedo and insulation: Fig. 15 shows the optimal solutions and net savings for the new building insulation and albedo design. The net savings of optimizing both insulation and albedo for the new building were 2.20×10^4 CNY, approximately 5.6 times that of optimizing the insulation only and 1.6 times that of optimizing the albedo only. The optimal solution is that all the EPS thickness of walls and a roof reduced from 3.3 mm to 36.8 mm while the envelope albedos increased to the corresponding highest aged albedo. The EPS in the roof was reduced most, followed by the north, south, east, and west walls.

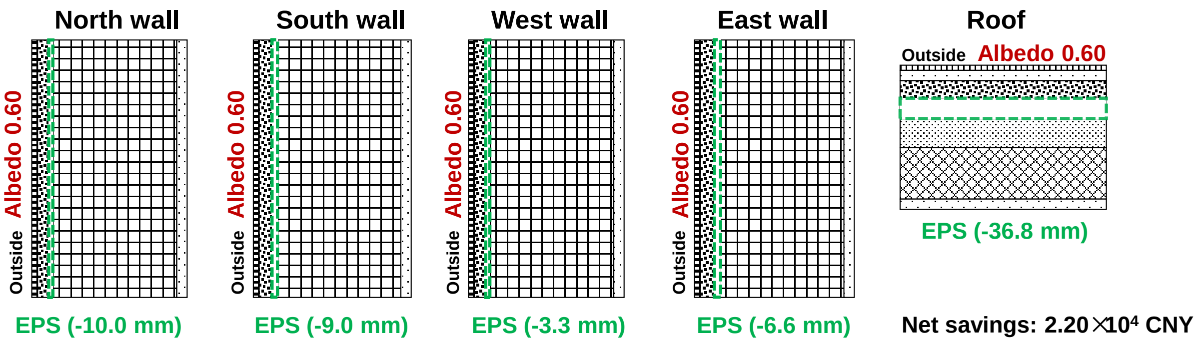

Fig. 15. Optimal EPS thickness, albedo, and net savings for the new building by optimizing both the albedo and insulation.

4 Discussion

Since 2012, cool envelopes have been given credits in the national design standards in hot summer climate zones in China [52][53]. In the context of prescriptive standards, a "credit" is a trade-off that allows more flexibility in the building design. For instance, a cool envelope credit might permit less insulation in the envelope assembly [54]. Current standards have standardized and recommended cool coatings applications on building envelopes, offering energy-saving-oriented design solutions for buildings. It is also recommended in standard JGJ/T 129-2012 *Technical specification for energy efficiency retrofitting of existing residential buildings* [55] to adopt cool coatings in retrofitting the existing roofs for residential buildings in hot summer and warm winter climate zones. However, through the investigation in this study, some suggestions and recommendations are provided:

(1) Standardized and specific retrofitting requirements of cool envelopes should be further included in the technical norms. It is found that some options can be energy-effective but not always be cost-effective. Therefore, the retrofit decisions of building envelopes should be made based on life cycle cost assessment, taking account of the envelope construction, building vintage, orientation, and neighboring shading. For example, when retrofitting newly constructed buildings, although cool roofs and cool walls yield energy savings, the 20-year net savings is negative due to the high envelope insulation.

(2) Given the demonstrated potential benefits of cool-coated office buildings in Hot Summer regions, the insulation of all building envelopes prescribed by the current design standard (GB 50189-2015 *Design standard for energy efficiency of public buildings of China* [27]) can be reduced to achieve the maximum net savings of building envelope design. This standard implies that cool envelopes should be properly integrated into building design practices and standards.

(3) To ensure cool walls' applicability, it is imperative to take account of the shading and

reflection by neighboring buildings and reflection from the ground comprehensively. Therefore, the application of cool coatings on building clusters or communities is also a challenge to be addressed.

(4) In a megacity like Chongqing, although it has high population density and likely high production of particulate matter from various sources, the albedo of cool roofs can still higher than 0.55 after 1-year of natural exposure [56]. For cool wall products, 1-year albedo losses are slightly lower than that of cool roof products [39]. As most of the decrease in the albedo of cool surfaces occurs in the first year and then the albedo tends to be stabilized [21], brand new cool surfaces are assumed to have a stabilized albedo of 0.6 after natural aging, soiling, or weathering in this study. However, further studies may be required to explore the potential benefits of cool-coated buildings by taking dynamic albedo variations of cool surfaces over the life cycle into consideration. The soiling and weathering characteristics of cool coatings need further investigation through long-term monitoring.

5 Conclusions

This study proposes a holistic approach integrating field testing, building energy simulation, and a 20-year life-cycle-based optimization to explore the maximum potential benefits of cool-coated buildings and the maximum net savings achieved by the optimal retrofit or design of building envelopes. Based on the results of the case study, the following conclusions can be made.

- The experimental results show that applying cool coatings on the wall can significantly reduce the exterior surface temperature. During the test period, the cool west wall was up to 9.3 °C cooler than the gray west wall.
- Applying cool coatings on old buildings (with high thermal transmittance) has higher potential benefits than new buildings (with low thermal transmittance). The annual energy simulation results show that cool envelopes reduced conduction heat gain per unit modified area by 20.2 – 62.1 kWh/m^2 in old buildings and 5.2 – 23.6 kWh/m^2 in new buildings. Cool envelopes lowered the annual HVAC electricity use per unit modified area by 1.9 to 7.1 kWh/m^2 in old buildings and 0.9 to 1.4 kWh/m^2 in new buildings. Adding cool coatings on whole building envelopes could achieve 11.9% and 5.9% electricity savings annually for old and new buildings, respectively.
- Retrofitting old buildings with a cool roof provided the 20-year net savings per modified area with present values up to 42.8 CNY/m^2, while retrofitting a new building with a cool

roof or cool walls was not cost-effective. If the original coatings on facets are at the end-of-service-life, it is recommended to retrofit all building envelopes with cool coatings to achieve a 20-year net savings per unit modified area with present values of 44.6 CNY/m^2 and 13.6 CNY/m^2 for old buildings and new buildings, respectively.

- The optimal design of building envelope through optimizing both insulation and albedo can provide the building owners with the highest economic benefit, which is 5.6 times the net savings of optimizing the insulation only and 1.6 times that of optimizing albedo only.

Acknowledgments

This research work was supported by the National Natural Science Foundation of China (No. 51878088) and the IEA EBC Annex 80 Resilient Cooling. It was also supported by the Assistant Secretary for Energy Efficiency and Renewable Energy, Building Technologies Office of the U.S. Department of Energy under Contract No. DE-AC02-05CH11231.

Appendix A Map of China's climate zone

Fig. A-16 shows the overall layout of China's five climate zones: severe cold A, severe cold B, cold, hot summer/cold winter, and hot summer/warm winter.

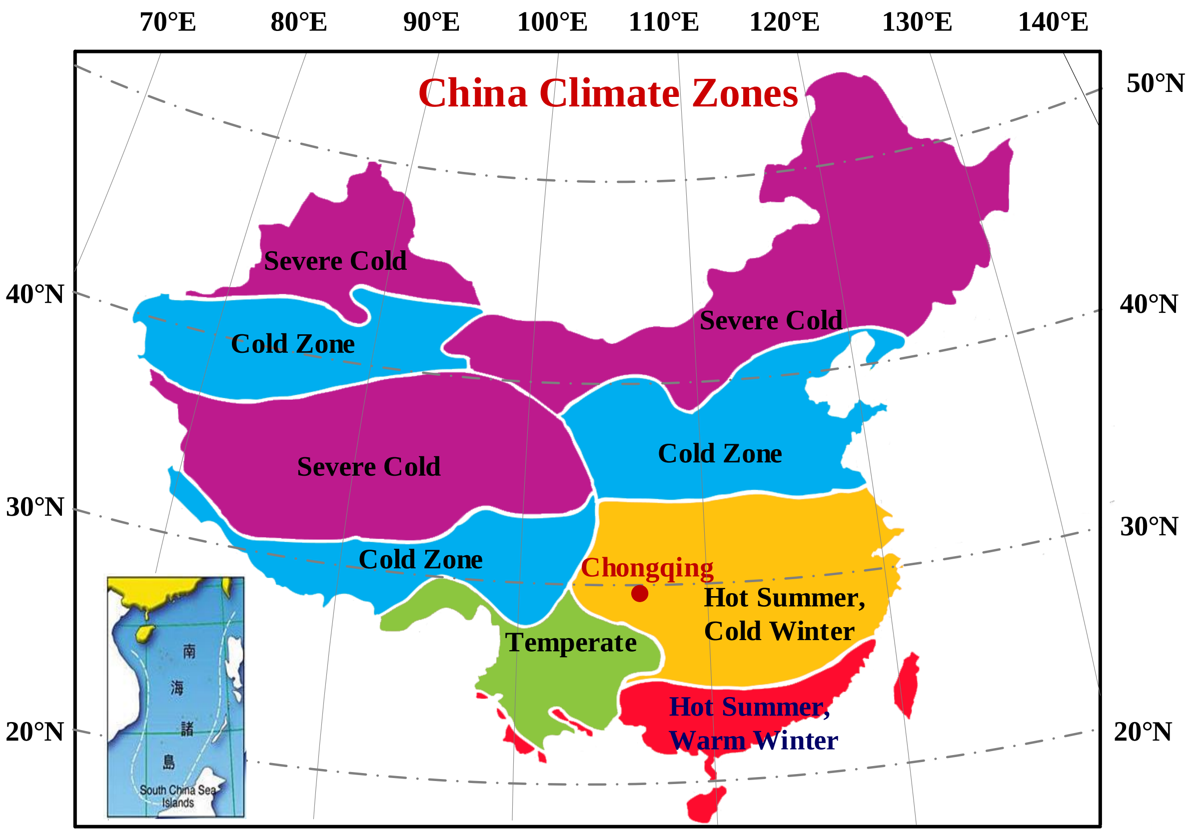

Fig. A-16. Map of China's climate zone [57].

References

[1] U. Eicker, Low energy cooling for sustainable buildings, John Wiley & Sons, 2009. https://www.wiley.com/en-us/Low+Energy+Cooling+for+Sustainable+Buildings-p-9780470697443.

[2] R. Guo, Y. Gao, C. Zhuang, P. Heiselberg, R. Levinson, X. Zhao, D. Shi, Optimization of cool roof and night ventilation in office buildings: A case study in Xiamen, China, Renew. Energy. 147 (2020) 2279–2294. https://doi.org/10.1016/j.renene.2019.10.032.

[3] J. Lei, K. Kumarasamy, K.T. Zingre, J. Yang, M.P. Wan, E.H. Yang, Cool colored coating and phase change materials as complementary cooling strategies for building cooling load reduction in tropics, Appl. Energy. (2017). https://doi.org/10.1016/j.apenergy.2016.12.114.

[4] R. Levinson, H. Akbari, Potential benefits of cool roofs on commercial buildings: Conserving energy, saving money, and reducing emission of greenhouse gases and air pollutants, Energy Effic. (2010). https://doi.org/10.1007/s12053-008-9038-2.

[5] K.T. Zingre, M.P. Wan, S.K. Wong, W.B.T. Toh, I.Y.L. Lee, Modelling of cool roof performance for double-skin roofs in tropical climate, Energy. (2015). https://doi.org/10.1016/j.energy.2015.01.092.

[6] Y. Gao, J. Xu, S. Yang, X. Tang, Q. Zhou, J. Ge, T. Xu, R. Levinson, Cool roofs in China: Policy review, building simulations, and proof-of-concept experiments, Energy Policy. 74 (2014) 190–214. https://doi.org/10.1016/j.enpol.2014.05.036.

[7] T. Xu, J. Sathaye, H. Akbari, V. Garg, S. Tetali, Quantifying the direct benefits of cool roofs in an urban setting: Reduced cooling energy use and lowered greenhouse gas emissions, Build. Environ. 48 (2012) 1–6. https://doi.org/10.1016/j.buildenv.2011.08.011.

[8] J.S. Haberl, S. Cho, Literature Review of Uncertainty of Analysis Methods,(DOE-2 Program), Report to the Texas Commission on Environmental Quality, (2004). https://oaktrust.library.tamu.edu/handle/1969.1/2072.

[9] A. Synnefa, M. Santamouris, H. Akbari, Estimating the effect of using cool coatings on energy loads and thermal comfort in residential buildings in various climatic conditions, Energy Build. 39 (2007) 1167–1174. https://doi.org/10.1016/j.enbuild.2007.01.004.

[10] V. Costanzo, G. Evola, L. Marletta, Cool roofs for passive cooling: performance in

different climates and for different insulation levels in Italy, Adv. Build. Energy Res. 7 (2013) 155–169. https://doi.org/10.1080/17512549.2013.865556.

[11] D. Kolokotsa, C. Diakaki, S. Papantoniou, A. Vlissidis, Numerical and experimental analysis of cool roofs application on a laboratory building in Iraklion, Crete, Greece, Energy Build. 55 (2012) 85–93. https://doi.org/10.1016/j.enbuild.2011.09.011.

[12] P.J. Rosado, R. Levinson, Potential benefits of cool walls on residential and commercial buildings across California and the United States: Conserving energy, saving money, and reducing emission of greenhouse gases and air pollutants, Energy Build. 199 (2019) 588–607. https://doi.org/10.1016/j.enbuild.2019.02.028.

[13] J. Zhang, A. Mohegh, Y. Li, R. Levinson, G. Ban-Weiss, Systematic Comparison of the Influence of Cool Wall versus Cool Roof Adoption on Urban Climate in the Los Angeles Basin, Environ. Sci. Technol. 52 (2018) 11188–11197. https://doi.org/10.1021/acs.est.8b00732.

[14] H. Shen, H. Tan, A. Tzempelikos, The effect of reflective coatings on building surface temperatures, indoor environment and energy consumption - An experimental study, Energy Build. 43 (2011) 573–580. https://doi.org/10.1016/j.enbuild.2010.10.024.

[15] W. Guo, X. Qiao, Y. Huang, M. Fang, X. Han, Study on energy saving effect of heat-reflective insulation coating on envelopes in the hot summer and cold winter zone, Energy Build. 50 (2012) 196–203. https://doi.org/10.1016/j.enbuild.2012.03.035.

[16] K. Saafi, N. Daouas, A life-cycle cost analysis for an optimum combination of cool coating and thermal insulation of residential building roofs in Tunisia, Energy. 152 (2018) 925–938. https://doi.org/10.1016/j.energy.2018.04.010.

[17] J. Sproul, M.P. Wan, B.H. Mandel, A.H. Rosenfeld, Economic comparison of white, green, and black flat roofs in the United States, Energy Build. 71 (2014) 20–27. https://doi.org/10.1016/j.enbuild.2013.11.058.

[18] D. Shi, Y. Gao, R. Guo, R. Levinson, Z. Sun, B. Li, Life cycle assessment of white roof and sedum-tray garden roof for office buildings in China, Sustain. Cities Soc. 46 (2019). https://doi.org/10.1016/j.scs.2018.12.018.

[19] R.S. Arumugam, V. Garg, V.V. Ram, A. Bhatia, Optimizing roof insulation for roofs with high albedo coating and radiant barriers in India, J. Build. Eng. 2 (2015) 52–58. https://doi.org/10.1016/j.jobe.2015.04.004.

[20] C. Piselli, A.L. Pisello, M. Saffari, A. de Gracia, F. Cotana, L.F. Cabeza, Cool roof impact on building energy need: The role of thermal insulation with varying climate conditions, Energies. 12 (2019) 3354. https://doi.org/10.3390/en12173354.

[21] S.E. Bretz, H. Akbari, Long-term performance of high-albedo roof coatings, Energy Build. 25 (1997) 159–167. https://doi.org/10.1016/s0378-7788(96)01005-5.

[22] M. Sleiman, G. Ban-Weiss, H.E. Gilbert, D. François, P. Berdahl, T.W. Kirchstetter, H. Destaillats, R. Levinson, Soiling of building envelope surfaces and its effect on solar reflectance - Part I: Analysis of roofing product databases, Sol. Energy Mater. Sol. Cells. 95 (2011) 3385–3399. https://doi.org/10.1016/j.solmat.2011.08.002.

[23] A. Material, Pausing for reflection on aging of the cool roof, J. Archit. Coatings. (2008) 63–66. https://www.paintsquare.com/library/articles/Durability_Pausing_for_reflection_on_aging_of_the_cool_roof.pdf.

[24] Y. Jiang, X. Wu, Annual report on China building energy efficiency, China Archit. Build. Press. Beijing (in Chinese). (2015). https://www.energycharter.org/fileadmin/DocumentsMedia/EERR/EER-China_ENG.pdf.

[25] IEA (International Energy Agency), The future of cooling in China, Paris, 2019. https://www.iea.org/reports/the-future-of-cooling-in-china.

[26] GB 50189-93 Thermal design for tourism hotel, Ministry of Housing and Urban-Rural Development, People's Republic of China, 1993.

[27] GB 50189-2015 Design standard for energy efficiency of public buildings, Ministry of Housing and Urban-Rural Development, People's Republic of China, 2015.

[28] GB 50189-2005 Design standard for energy efficiency of public buildings, Ministry of Housing and Urban-Rural Development, People's Republic of China, 2005.

[29] Y. Min, Y. Chen, W. Shi, H. Yang, Applicability of indirect evaporative cooler for energy recovery in hot and humid areas: Comparison with heat recovery wheel, Appl. Energy. 287 (2021) 116607. https://doi.org/10.1016/j.apenergy.2021.116607.

[30] T. Hong, C. Li, D. Yan, Updates to the China Design Standard for Energy Efficiency in public buildings, Energy Policy. 87 (2015) 187–198. https://doi.org/10.1016/j.enpol.2015.09.013.

[31] D.B. Crawley, L.K. Lawrie, F.C. Winkelmann, W.F. Buhl, Y.J. Huang, C.O. Pedersen, R.K. Strand, R.J. Liesen, D.E. Fisher, M.J. Witte, J. Glazer, EnergyPlus: Creating a new-generation building energy simulation program, Energy Build. 33 (2001) 319–331. https://doi.org/10.1016/S0378-7788(00)00114-6.

[32] GB/T9755-2001: Synthetic resin emulsion coatings for exterior wall., General Administration of Quality Supervision, People's Republic of China, 2001.

[33] A. Synnefa, M. Saliari, M. Santamouris, Experimental and numerical assessment of the impact of increased roof reflectance on a school building in Athens, in: Energy Build., Elsevier, 2012: pp. 7–15. https://doi.org/10.1016/j.enbuild.2012.01.044.

[34] C. Zhuang, K. Shan, S. Wang, Coordinated demand-controlled ventilation strategy for energy-efficient operation in multi-zone cleanroom air-conditioning systems, Build. Environ. 191 (2021) 107588. https://doi.org/10.1016/j.buildenv.2021.107588.

[35] R. Guo, Y. Hu, M. Liu, P. Heiselberg, Influence of design parameters on the night ventilation performance in office buildings based on sensitivity analysis, Sustain. Cities Soc. 50 (2019) 101661. https://doi.org/10.1016/j.scs.2019.101661.

[36] S. Moslehi, T.A. Reddy, S. Katipamula, Evaluation of data-driven models for predicting solar photovoltaics power output, Energy. (2018). https://doi.org/10.1016/j.energy.2017.09.042.

[37] J.S. Haberl, D.E. Claridge, C. Culp, ASHRAE's Guideline 14-2002 for Measurement of Energy and Demand Savings: How to Determine What Was Really Saved by the Retrofit, 2005. https://oaktrust.library.tamu.edu/handle/1969.1/5147.

[38] WMO Country Profile Database, World Meteorological Organization, (2018). https://www.wmo.int/cpdb/.

[39] R. Levinson, G. Ban-Weiss, P. Berdahl, S. Chen, H. Destaillats, N. Dumas, H. Gilbert, H. Goudey, S. Houzé de l'Aulnoit, J. Kleissl, B. Kurtz, Y. Li, Y. Long, A. Mohegh, N. Nazarian, M. Pizzicotti, P. Rosado, M. Russell, J. Slack, X. Tang, J. Zhang, W. Zhang, Solar-Reflective "Cool" Walls: Benefits, Technologies, and Implementation (CEC-500-2019-040; also LBNL-2001296), 2019. https://doi.org/10.20357/B7SP4H.

[40] Mathworks, Parallel Computing Toolbox, User's Documentation R2019b, The MathWorks Inc.,Massachusetts, 2019. https://www.mathworks.com/help/parallel-computing/index.

[41] M. Mossolly, K. Ghali, N. Ghaddar, Optimal control strategy for a multi-zone air conditioning system using a genetic algorithm, Energy. (2009). https://doi.org/10.1016/j.energy.2008.10.001.

[42] P.D. Lavappa, J.D. Kneifel., Energy Price Indices and Discount Factors for Life-Cycle Cost Analysis – 2020 Annual Supplement to NIST Handbook 135, 2020. https://doi.org/10.6028/NIST.IR.85-3273-35.

[43] Power grid sales price list in Chongqing, Retrieved from State Grid Corp. China, People's Repub. China State Grid Corp. China. (2018). http://www.sgcio.com/Banksinfo/fangan/74265.html.

[44] B. Urban, K. Roth, Guidelines for selecting cool roofs, US Department of Energy, Washington, DC, 2010. https://www.energy.gov/eere/femp/downloads/guidelines-selecting-cool-roofs.

[45] ENERGY STAR, Roof Products Key Product Criteria, (2007). https://www.energystar.gov/products/building_products/roof_products/key_product_criteria.

[46] Stephen C. Plotner, Building Construction Cost Data 2016, 74th annua, Rockland, MA: RSMeans, 2015. https://books.google.dk/books?id=LCB6jgEACAAJ.

[47] Y. Hang, M. Qu, R. Winston, L. Jiang, B. Widyolar, H. Poiry, Experimental based energy performance analysis and life cycle assessment for solar absorption cooling system at University of Californian, Merced, Energy Build. 82 (2014) 746–757. https://doi.org/10.1016/j.enbuild.2014.07.078.

[48] Mathworks, Global Optimization Toolbox, User's Documentation R2019b, The MathWorks Inc.,Massachusetts, 2019. https://www.mathworks.com/help/gads/index.

[49] U.S. Department of Energy, EnergyPlus 9.3 Engineering Reference, (2020). https://bigladdersoftware.com/epx/docs/9-3/engineering-reference/.

[50] J. Torriti, M.G. Hassan, M. Leach, Demand response experience in Europe: Policies, programmes and implementation, Energy. (2010). https://doi.org/10.1016/j.energy.2009.05.021.

[51] M. Hu, F. Xiao, Price-responsive model-based optimal demand response control of inverter air conditioners using genetic algorithm, Appl. Energy. 219 (2018) 151–164. https://doi.org/10.1016/j.apenergy.2018.03.036.

[52] JGJ 75-2012 Design standard for energy efficiency of residential buildings in hot summer and warm winter zone, Ministry of Housing and Urban-Rural Development, People's Republic of China, 2012.

[53] GB/T 50378-2014 Assesment standard for green building, Ministry of Housing and Urban-Rural Development, People's Republic of China, 2014.

[54] J. Ge, R.M. Levinson, The Advancement of Cool Roof Standards in China from 2010 to 2015. Report LBNL-1007007, Lawrence Berkeley National Lab, Berkeley, CA (United States), 2016. https://www.osti.gov/servlets/purl/1361499.

[55] JGJ/T 129-2012 Technical specification for energy efficiency retrofitting of existing residential buildings, Ministry of Housing and Urban-Rural Development, People's Republic of China, 2012.

[56] Y. Gao, D. Shi, R. Levinson, R. Guo, C. Lin, J. Ge, Thermal performance and energy savings of white and sedum-tray garden roof: A case study in a Chongqing office building, Energy Build. 156 (2017) 343–359. https://doi.org/10.1016/j.enbuild.2017.09.091.

[57] GB50176-93 Thermal Design Code for Civil Building, Ministry of Housing and Urban-Rural Development, People's Republic of China, 1993.